COPI mediates recycling of an exocytic SNARE from endosomes by recognition of a ubiquitin sorting signal

Peng Xu[1], Hannah M. Hankins[1], Chris Macdonald[2], Samuel J. Erlinger[1], Meredith N. Frazier[1], Nicholas S. Diab[1], Robert C. Piper[2], Lauren P. Jackson[1], Jason A. MacGurn[3] and Todd R. Graham[1*]

[1]Department of Biological Sciences, Vanderbilt University, Nashville, TN 37235, USA

[2]Department of Molecular Physiology and Biophysics, University of Iowa, Iowa City, IA 52242, USA

[3]Department of Cell and Developmental Biology, Vanderbilt University Medical Center, Nashville, TN 37235, USA

*Correspondence to: email: tr.graham@vanderbilt.edu

ABSTRACT

The COPI coat forms transport vesicles from the Golgi complex and plays a poorly defined role in endocytic trafficking. Here we show that COPI mediates delivery of a budding yeast SNARE (Snc1) from early endosomes to the Golgi complex through recognition of a polyubiquitin sorting signal. Snc1 is a v-SNARE that drives fusion of exocytic vesicles with the plasma membrane, and then recycles through early endosomes back to the Golgi for reuse. Removal of ubiquitin from Snc1, or deletion of a β'-COP subunit propeller domain that binds K63-linked polyubiquitin, causes aberrant accumulation of Snc1 in early endosomes. Moreover, replacement of the β'-COP propeller domain with unrelated ubiquitin-binding domains restores Snc1 recycling. These results indicate that ubiquitination, a modification well known to target membrane proteins to the lysosome or vacuole for degradation, can also function as recycling signal to sort a SNARE into COPI vesicles at early endosomes for Golgi delivery.

INTRODUCTION

Sequential rounds of vesicle budding and fusion reactions drive protein transport through the secretory and endocytic pathways (Rothman, 1994). Vesicle budding often requires cytosolic coat proteins, such as COPI, COPII or clathrin, that assemble onto the donor organelle to mold the membrane into a tightly curved structure while collecting cargo for inclusion into the nascent vesicle (Faini et al., 2013). Efficient departure of cargo from the donor organelle requires a sorting signal within the protein that is recognized by the coat complexes. For example, the heptameric COPI coat complex assembles onto Golgi membranes where it selects cargo bearing a C-terminal di-lysine (KKxx-COO^- or KxKxx-COO^-) sorting signal exposed on the cytosolic side of the membrane (Eugster et al., 2004; Letourneur et al., 1994; Waters et al., 1991). The two large COPI subunits, α- and β'-COP, each contain a pair of WD40 repeat domains that form twin β-propellers used to select cargo by binding to the sorting signal (Jackson, 2014; Jackson et al., 2012). After budding, COPI vesicles uncoat and deliver the di-lysine bearing cargo to the ER by fusing to this acceptor membrane in a SNARE-dependent reaction (Rein et al., 2002; Sudhof and Rothman, 2009).

Intrinsic to the SNARE hypothesis is the privileged selection of v-SNAREs (also called R-SNAREs) by the vesicle budding machinery to ensure the nascent vesicle can fuse to its target membrane bearing complementary t-SNAREs (Q-SNAREs), and the subsequent need for v-SNARE recycling back to the donor compartment (Miller et al., 2011). v-SNAREs are small, single-pass membrane proteins with the C-terminus embedded within the lumenal space (Weber et al., 1998). Thus, COPI cannot select v-SNAREs using the canonical C-terminal motifs and there is no known sorting signal within a v-SNARE that is recognized by COPI. A further complication with the vesicular transport process is that it leads to depletion of v-SNAREs from the donor membrane and their deposition in the acceptor membrane. Thus, it is essential to recycle the v-SNAREs back to the donor compartment in order to sustain the vesicular transport pathway. Exocytic v-SNAREs that bud from the trans-Golgi network and target vesicles to the plasma membrane have served as models to understand the mechanisms of SNARE recycling, although these studies have primarily focused on how the v-SNAREs are endocytosed from the plasma membrane for delivery to early endosomes (Burston et al., 2009; Lewis et al., 2000; Miller et al., 2011). The subsequent step of transport from endosomes back to the Golgi, however, is poorly understood.

In the case of the yeast exocytic v-SNARE Snc1, recycling from endosomes back to the Golgi is independent of retromer and clathrin adaptors known to mediate transport of other cargos in these pathways (Lewis et al., 2000). Instead, an F-box protein (Rcy1) (Galan et al., 2001), a phosphatidylserine flippase (Drs2) (Hua et al., 2002; Xu et al., 2013), an ArfGAP (Gcs1) (Robinson et al., 2006) and a sorting nexin complex (Snx4/41) (Lewis et al., 2000; Ma et al., 2017) are required for endosome to Golgi transport of Snc1, although the precise functions for these proteins remain unclear. F-box proteins are best known as substrate-selecting adaptors in Skp1-Cullin-F-box (SCF) E3 ubiquitin (Ub) ligases, but the Rcy1-Skp1 complex plays a role in Snc1 recycling that is independent of the cullin subunit or the Cdc34 E2 Ub ligase (Galan et al., 2001). Moreover, ubiquitination of membrane proteins in the endocytic pathway is thought to set a course for their degradation in the lysosome or vacuole via the ESCRT/MVB pathway (MacGurn et al., 2012). Thus, it seemed unlikely that Rcy1 mediates ubiquitination of Snc1 in order to recycle this SNARE protein out of the endocytic pathway. Nonetheless, several high-throughput studies have shown that Snc1 is ubiquitinated (Peng et al., 2003; Silva et al., 2015; Swaney et al., 2013), and altering a targeted lysine to arginine (Snc1-K63R) surprisingly perturbed its early endosome (EE) to TGN transport (Chen et al., 2011), suggesting ubiquitin (Ub) conjugation could play a role in Snc1 recycling.

Here we show that K63-linked polyubiquitin (polyUb) chains are indeed a sorting signal that drives EE to TGN transport of Snc1, and surprisingly find that COPI mediates this sorting event by direct binding to the polyUb chain. COPI was observed to localize to EEs in mammalian cells more than two decade ago (Aniento et al., 1996; Whitney et al., 1995), but had not previously been shown to localize to EEs in yeast. In addition, COPI was initially thought to mediate transport of proteins from EE to late endosomes in animal cells (Aniento et al., 1996). However, as models for early to late endosome maturation emerged (Scott et al., 2014; Zerial and McBride, 2001), this proposed role for endosomal COPI was abandoned and there remains no clearly defined role for COPI in protein trafficking through the endosomal system. A major impediment to deciphering a function for endosomal COPI is that mutations or knockdown approaches that inactivate COPI grossly disrupt Golgi function. Thus, any endosomal defects observed in COPI-deficient cells could be attributed to an indirect downstream effect of perturbing the Golgi complex. To demonstrate a direct functional role of COPI at endosomes would require specific mutations or variants of COPI that disrupt trafficking through the endosomes while maintaining its function at

the Golgi. We describe here a set of COPI separation-of-function mutations and fusion proteins that allow us to demonstrate a direct role of this coat at EEs to select cargo bearing K63-linked Ub chains.

RESULTS

Snc1 ubiquitination is required for EE to TGN transport.

Snc1 is an exocytic v-SNARE that is incorporated into vesicles budding from the *trans*-Golgi network (TGN) to drive fusion of these vesicles with the plasma membrane (Gerst et al., 1992). Afterwards, Snc1 is endocytosed, delivered to an early endosome population marked by the t-SNARE Tlg1 and then delivered back to the TGN for reuse in exocytosis (Lewis et al., 2000; Robinson et al., 2006). In wild-type (WT) cells, nearly half of GFP-Snc1 localizes to the plasma membrane (preferentially at the buds relative to the mother cell) and the remainder is observed in early endosomes and Golgi cisternae, which appear as small punctae (Figure 1A, B). As previously shown (Lewis et al., 2000), deletion of *RCY1* (*rcy1*Δ) disrupts EE to TGN transport of GFP-Snc1 causing its accumulation in early endosomal punctae and a loss from the plasma membrane (Figure 1A, B). Snc1 is ubiquitinated and a lysine mutation that reduces ubiquitination also caused GFP-Snc1 accumulation in EE punctae (Chen et al., 2011), suggesting that Ub could be a retrieval signal. However, lysines are commonly found in protein sorting signals, undergo a variety of other post-translational modifications, and serve structural roles, so it was unclear whether it was the loss of lysine or ubiquitination *per se* that caused the Snc1 recycling defect.

To address whether ubiquitination is required for Snc1 recycling, we fused the UL36 deubiquitinase (DUB) from Herpes simplex virus (Stringer and Piper, 2011), as well as a catalytically inert mutant (DUB*), to GFP-Snc1. This DUB can effectively strip Ub from a fusion partner without altering the amino acid sequences targeted for ubiquitination (Stringer and Piper, 2011). In contrast to GFP-Snc1, DUB-GFP-Snc1 localized to puncta marked by the EE/TGN protein Tlg1. In addition, DUB-GFP-Snc1 mislocalized to EEs of WT cells to the same extent as GFP-Snc1 mislocalized to EEs in *rcy1*Δ cells (Figure 1A-D). Deubiquitinase activity was required to block recycling as DUB*-GFP-Snc1 localized normally to the plasma membrane (Figure 1A-

D). To determine if localization of DUB-GFP-Snc1 to endosomes required endocytosis, we mutated the Snc1 endocytic internalization signal in the context of the DUB and DUB* fusion proteins (Lewis et al., 2000). The endocytosis-defective variants (e.g. DUB-GFP-Snc1-PM) accumulated at the plasma membrane (Figure 1A-D), indicating that the DUB disrupted early endosome to TGN trafficking rather than TGN to plasma membrane transport when attached to WT Snc1. These data imply that ubiquitination of Snc1 is required for EE to TGN transport, but has no effect on TGN to plasma membrane transport or endocytosis.

It was possible that the DUB interfered with Snc1 trafficking by deubiquitinating the trafficking machinery required for EE to TGN transport rather than solely deubiquitinating Snc1 itself. As a further test for the specificity of the DUB block in Snc1 recycling, we also attached DUB and DUB* to Drs2, an integral membrane phosphatidylserine flippase that localizes to the TGN and EE, and is part of the machinery required for EE to TGN transport of GFP-Snc1. Whereas GFP-Snc1 accumulated in EEs of *drs2*Δ cells, recycling to the plasma membrane was fully restored in *drs2*Δ cells expressing Drs2-DUB or Drs2-DUB* (Figure 1E-F). Thus, attaching DUB to a component of the trafficking machinery in this pathway has no effect on Snc1 recycling, implying that the DUB is not significantly acting on neighboring proteins within this pathway.

Snc1 is extensively modified with K63-linked polyUb chains

The high throughput studies that identified ubiquitinated Snc1 peptides did not distinguish whether it was modified with monoUb or polyUb. A prior study identified a mono-ubiquitinated form of Snc1 (Chen et al., 2011), which we confirmed, but we also found evidence for Snc1 forms heavily modified with polyUb (Figure 2A). We further found that poly-ubiquitinated HA-Snc1 is precipitated with ligands (Tandem Ubiquitin Binding Entities, TUBEs) specific for K63-linked polyUb but not for K48-linked polyUb (Figure 2B). This is consistent with the observation that Snc1 ubiquitination is significantly reduced in yeast strains expressing K63R ubiquitin as the sole source of Ub, and thus cannot generate K63-linked chains (Silva et al., 2015). We conclude that Snc1 is primarily modified with K63-linked poly-Ub.

Rcy1 is required for Snc1 recycling and was implicated in Snc1 ubiquitination. Therefore, we tested whether DUB fusion to this F-box protein would perturb GFP-Snc1 recycling. Attachment of DUB to the N-terminus of Rcy1 (as the sole source of this protein) did cause a partial defect in GFP-Snc1 recycling; however, the DUB* fusion protein caused the same partial

defect. Therefore, the DUB-Rcy1 fusions partially disrupted Rcy1 function by a mechanism that is independent of deubiquitinase activity (Figure 2C, D), which further emphasizes the specificity of the effect of DUB when fused to GFP-Snc1. To identify other ligases potentially acting on Snc1, we screened through a collection of E3 ligase-DUB fusion proteins (MacDonald et al., 2017) to see if any disrupted GFP-Snc1 recycling. DUB fusions with two endosome-localized E3 Ub ligases, Pib1 and Tul1, strongly perturbed GFP-Snc1 recycling (Figure 2E), while DUB fusion with the Rsp5 and Vps11 E3 ligases were without effect. Moreover, we immunoprecipitated untagged Snc1 from cells expressing Pib1-DUB and found that ubiquitination of Snc1 was reduced relative to Snc1 from the control strain (Figure 2F). We then tested the *pib1*Δ and *tul1*Δ single mutants, which were without phenotype, but the *pib1*Δ *tul1*Δ double mutant displayed a GFP-Snc1 recycling defect (Figure 2G,H). These results suggest that Pib1 and Tul1, rather than Rcy1, are primarily responsible for Snc1 ubiquitination.

COPI binds K63-linked polyUb directly and this interaction is required for GFP-Snc1 recycling

Given that Snc1 ubiquitination is critical for its recycling, we hypothesized that Ub conjugated to Snc1 may function as a sorting signal for endosome-to-TGN traffic and we asked what trafficking machinery might recognize Ub as a TGN retrieval sorting determinant. Inactivation of COPI using a temperature conditional allele (*ret1-1*) blocked GFP-Snc1 recycling, whereas clathrin adaptor mutants and retromer mutants had no effect (Figure 2- figure supplement 1) (Lewis et al., 2000; Robinson et al., 2006). However, the Golgi is markedly perturbed when COPI is inactivated, undermining clear interpretation of this result due to possible indirect effects of disrupting the Golgi. If COPI plays a direct role in Ub-dependent Snc1 transport from the endosome, we reasoned it might bind the Ub sorting signal and the endosomal Snc1 recycling function should be independent of established COPI functions at the Golgi complex.

COPI is a heptamer composed of a B-subcomplex (α/β'/ε-COP subunits) structurally similar to clathrin heavy chains (Figure 3A), and an F-subcomplex similar to tetrameric clathrin adaptors (not shown) (Dodonova et al., 2015; Faini et al., 2013; Fiedler et al., 1996). The α- and β'-COP subunits in the B-subcomplex each have two WD40 repeat propeller domains at their N-termini that bind dilysine sorting motifs. All well-characterized sorting signals recognized by COPI are near the C-terminus of the cargo and the N-terminal propellers of α and β'-COP use a

basic patch to coordinate the carboxyl group (Jackson, 2014). However, many WD40 repeat domains also bind Ub (Pashkova et al., 2010). Therefore, we examined COPI WD40 propeller domains for interaction with Ub and found that they bound to K63-linked tetraUb (K63 Ub_4) (Figure 3B). The N-terminal propeller of β'-COP (1-304) bound slightly better to Ub_4 than the first propeller of α-COP (1-327), and a fragment of β' carrying both propellers (1-604) bound most efficiently.

Binding of β'-COP propellers to Ub was remarkably specific for linkage and chain-length. Polymers containing 5 or more K63-linked Ubs were required for the most robust and specific binding (Figure 3C). In contrast, β'-COP (1-304) did not bind significantly to K48-linked Ub chains or mono-Ub (Figure 3C and Figure 3-figur supplement 1), and bound short K63-linked polymers poorly in this competitive binding experiment (Ub_2 - Ub_4) (Figure 3C, D). β'-COP (1-604), with both propellers, retained the same specificity but recovered greater amounts of polyUb in these GST pulldown assays (Figure 3C,D). These results demonstrate that the β'-COP and α-COP propeller domains can directly and specifically bind K63-linked poly-Ub.

To be certain that these Ub interactions were not an artifact of the recombinant GST fusion protein fragments assayed, we tested if the COPI complex isolated from yeast could bind polyUb. Extracts from yeast cells expressing HA-tagged or untagged (control) β'-COP as the sole source of this subunit were incubated with anti-HA beads to recover COPI. The majority of β'-COP in yeast is assembled into the heptameric COPI complex and these methods have been used previously to purify the full complex (Yip and Walz, 2011). The beads carrying COPI bound K63-linked polyUb, but not K48-linked polyUb, with the same chain length specificity as the individual propeller domains (Figure 3D-E). In contrast, the beads incubated with control lysate with untagged COPI did not bind any of the polyUb chains. These data indicate the full-length β'-COP binds K63-polyUb and suggests the full COPI complex binds as well.

We then tested if COPI propeller domains are required for recycling of GFP-Snc1. Cells expressing β'-COP harboring a deletion of the N-terminal propeller (Δ2-304) as the sole source of this subunit were viable but mislocalized GFP-Snc1 to Tlg1-marked compartments (Figure 4A-C). Deletion of the α-COP N-terminal propeller also disrupted Snc1 recycling, although not as severely (Figure 4A-C). The β'-COP N-terminal propeller contains a basic patch that binds to the C-terminus of cargos bearing specific variants of di-lysine sorting signals (e.g KxKxx-COO^-), such

as Emp47 (Eugster et al., 2004; Schroder-Kohne et al., 1998). Therefore, it was possible that the GFP-Snc1 recycling defect caused by β'-COP (Δ2-304) was a secondary effect of mislocalizing a subset of di-lysine cargos recognized preferentially by this propeller. Mutation of the di-lysine binding site (β'-COP RKR mutant: R15A K17A R59A) disrupts the di-lysine interaction and causes myc-Emp47 mislocalization to the vacuole where it is degraded (Eugster et al., 2004). By contrast, the β'-COP RKR mutant localized GFP-Snc1 normally to the plasma membrane (Figure 4A-C). Therefore, the GFP-Snc1 recycling defect of β'-COP (Δ2-304) was not due to the loss of the di-lysine binding site. Importantly, these separation-of-function mutations clearly show that the role of β'-COP at the Golgi in recognizing certain di-lysine signals can be unlinked from its role in recycling GFP-Snc1 from EEs.

Replacement of the β'-COP N-terminal WD40 domain with unrelated Ub-binding domains restores Snc1 recycling

To test if recognition of Ub is the critical function of β'-COP in Snc1 recycling, we replaced the N-terminal propeller domain with three different Ub-binding domains. The first is a β-propeller Ub-binding domain from Doa1 (UBD_{Doa1}) that has no significant sequence similarity to β'-COP, but is known to bind Ub without linkage or chain-length specificity (β'-COP UBD_{Doa1}) (Pashkova et al., 2010). The second is the Npl4 Zinc Finger (NZF) domain from Tab2, which binds specifically to K63-linked polyUb (Sato et al., 2009). The third is the K48-linkage specific UBA domain from Mud1 (Trempe et al., 2005). Strikingly, the UBD_{Doa1} and NZF_{Tab2} domains fully restored β'-COP function in GFP-Snc1 recycling (Figure 4A-C), but the UBA_{Mud1} domain failed to support this trafficking pathway. Importantly, COPI Ub binding appears to be conserved because human β'-COP (1-303) bound K63-linked polyUb comparably to the orthologous yeast domain (Figure 4-figure supplement 1A-C), and yeast cells expressing a chimeric yeast β'-COP with a human N-terminal propeller fully supported GFP-Snc1 trafficking (Figure 4A-D).

β'-COP is encoded by the *SEC27* gene, which is essential for yeast viability. All of the β'-COP chimeras and mutants described above supported the viability of yeast as the sole source of this subunit (Figure 4E). Therefore, all must be sufficiently well folded and functional to assemble into the heptameric complex. Interestingly, deletion of the β'-COP N-terminal propeller caused a slow growth phenotype that was fully rescued by its replacement with the general Ub-binding

domain from Doa1 (UBD_{Doa1}), or the human β'-COP N-terminal propeller. The β'-COP (RKR) di-lysine binding mutant also supports WT growth. These results suggest that the slow growth phenotype caused by β'-COP (Δ2-304) was due to loss of Ub binding but not di-lysine binding. In contrast, β'-COP NZF_{Tab2}, which binds K63-linked Ub, failed to correct the growth defect even though it fully restored GFP-Snc1 recycling (Figure 3A-D). The β'-COP UBA_{Mud1} chimera failed to correct the growth defect or Snc1 trafficking phenotypes exhibited by β'-COP (Δ2-304). The reason β'-COP NZF_{Tab2} and β'-COP UBD_{Doa1} influence growth differently is currently unclear, but suggest some COPI cargos may be modified with polyUb bearing linkages other than K63 or K48. These results also indicate that the growth and Snc1 trafficking defects can be uncoupled using different β'-COP variants.

It was possible that β'-COP (Δ2-304) destabilized the COPI coat and generally disrupted COPI function at the Golgi complex, thereby causing Snc1 recycling defects as a secondary consequence of perturbing the Golgi. Therefore, we examined the influence of these COPI variants on GFP-Rer1 cycling between the ER and Golgi complex. Rer1 is transported to the Golgi in COPII-coated vesicles and returned to the ER in COPI-coated vesicles, but displays a steady-state localization to early Golgi cisternae. Mutations that generally perturb COPI function, such as the temperature-sensitive *ret1-1* mutation in α-COP (Letourneur et al., 1994; Sato et al., 2001), mislocalize GFP-Rer1 to the vacuole (Figure 5A,B). Even at a permissive growth temperature of 27˚C, the *ret1-1* mutant displays significant mislocalization of Rer1-GFP to the vacuole (Fig 5A, B). By contrast, the β'-COP (Δ2-304), RKR and UBD_{Doa1} mutants all localized GFP-Rer1 to the Golgi as efficiently as WT cells (Figure 5A,B). The β'-COP N-terminal di-lysine binding site has a specific role in sorting Emp47 within the Golgi. As previously reported, β'-COP (Δ2-304) and the RKR mutant mislocalizes Emp47 to the vacuole where it is degraded (Eugster et al., 2004). Replacement of the N-terminal propeller of β'-COP with the NZF_{Tab1} or UBD_{Doa1} domains predictably failed to stabilize Myc-Emp47 because these domains lack the di-lysine binding site (Figure 5C). We conclude the ability of β'-COP to bind ubiquitin is crucial for Snc1 transport from EEs to the TGN, but has no role in the COPI-dependent trafficking of Rer1 or Emp47 at the Golgi complex. This collection of β'-COP fusion proteins provide an additional set of separation-of-function alleles that not only uncouple the roles of COPI at Golgi and endosomes, but also clearly demonstrate the importance of the COPI-Ub interaction *in vivo* for GFP-Snc1 recycling.

COPI localizes to Golgi and early endosome membranes in budding yeast

Our data indicate COPI has a distinct function in Snc1 recycling from early endosomes that is independent of its role at the Golgi, where most COPI is localized. While COPI has been localized to early endosomes of animal cells (Whitney et al., 1995), a pool of COPI at early endosomes in budding yeast has not been reported. Therefore, we quantified the colocalization of COPI-mKate with the early Golgi marker GFP-Rer1, the TGN and EE marker GFP-Tlg1, and the TGN-specific marker GFP-Sec7 (Figure 6A, B). While most COPI puncta colocalized with the early Golgi (61.3 +/- 6.3%), we found 18.4 +/- 3.6% of COPI co-localized with Tlg1, and only 2.5 +/- 1.4% colocalized with Sec7 (Figure 6A, B). These results indicate that the Tlg1-marked punctae decorated by COPI were primarily early endosomes rather than TGN. We also considered the possibility that Tlg1 was partially present in the early Golgi, which could provide an alternative explanation for the co-localization with COPI. However, colocalization between mCherry-Tlg1 and GFP-Rer1 was negligible (2.4 +/- 1.4%) (Figure 6A, B). Together, these data argue that COPI localizes to EEs and plays a direct role in sorting ubiquitinated cargo from EEs to the TGN.

DISCUSSION

Here we report that the COPI vesicle coat protein recognizes a ubiquitin sorting signal on the exocytic v-SNARE Snc1 and mediates the trafficking of this SNARE from early endosomes back to the TGN. The significance of these observations to the protein trafficking field is that they 1) contrast with prevailing views on the role of ubiquitin in the endocytic pathway, 2) define a new and unexpected sorting signal recognized by the COPI coat, 3) define a novel mechanism for v-SNARE recycling, and 4) help resolve a 20-year controversy over the role of COPI on endosomes.

The multifaceted roles of Ub in protein trafficking

This study challenges the assumption that ubiquitination of membrane proteins in the secretory or endocytic pathways will target the modified protein solely to the vacuole for degradation. Ubiquitin is well known to be a sorting signal recognized by clathrin adaptor proteins at the TGN and plasma membrane, and by the ESCRT complexes in the endosomal system. The clathrin adaptor interactions initially sort the ubiquitinated cargo into the endosomal system, while the ESCRTs mediate sorting into intraluminal vesicles of multivesicular bodies for eventual

delivery to vacuole (or lysosome) lumen where the cargo is typically degraded (MacGurn et al., 2012). In the yeast system, mono-ubiquitination of cargo appears to be sufficient to drive these sorting events (Stringer and Piper, 2011) and it is thought that ubiquitin would have to be removed from cargo by a deubiquitinase in order to rescue the protein from vacuolar delivery. In contrast, we show a physiologically relevant example for how *addition* of a K63-linked polyUb chain onto a SNARE serves as a COPI-dependent sorting signal that diverts this cargo away from the endocytic pathway and mediates its retrieval from early endosomes back to the TGN. A prior study had demonstrated that mutation of a conserved lysine in Snc1 (coincidentally K63) reduced its ubiquitination and perturbed recycling. However, it was possible that K63 in Snc1 was part of a more traditional lysine-based sorting signal in addition to being the primary target of ubiquitination. We rule out this possibility by the observation that fusion of a deubiquitinase (DUB) to GFP-Snc1 also disrupts its recycling without altering the Snc1 amino acid sequence. Our observation that COPI binds directly to K63-linked poly-Ub chains and this interaction is necessary for Snc1 recycling strongly supports the conclusion that Ub is the sorting signal in this pathway.

Our results provide a remarkable example of how the Ub code can be written and/or read in a spatiotemporally defined manner to control protein sorting decision points in the endocytic pathway. The Ub code is written by Ub ligases that determine the specific linkage and length of the Ub chains in competition with endogenous DUBs (Komander et al., 2009; MacGurn et al., 2012). The F-box protein Rcy1 has been implicated in Snc1 ubiquitination (Chen et al., 2011), but other SCF subunits are not required for Snc1 trafficking (Galan et al., 2001) and we find fusion of a DUB directly to Rcy1 does not perturb its function in this pathway. However, DUB fusion with endosomal E3 ligases Pib1 and Tul1 does disrupt Snc1 recycling, as does combined deletion of the *PIB1* and *TUL1* genes. Thus, Pib1 and Tul1 are good candidates for the E3 ligases that modify Snc1. This likely occurs at an early endosome population that lacks the ESCRT machinery so ubiquitinated Snc1 can be recycled by COPI rather than sorted into intraluminal vesicles. Conversely, it is possible that ESCRTs and COPI can compete for this cargo at the same compartment, but the length of the K63-linked polyUb chain on Snc1 determines whether COPI binds (long chains) or ESCRTs bind (mono or short chains). These events appear to be regulated because WT yeast harvested at a late phase of logarithmic growth display a substantial amount of GFP-Snc1 in the vacuole lumen (MacDonald et al., 2015). It will be interesting to determine if it

is a regulated change in the trafficking machinery, or extent of Snc1 ubiquitination that elicits this switch in the Snc1 destination.

K63-linked polyUb is a sorting signal that binds directly to COPI

COPI plays a major role in organelle biogenesis by helping establish the specific protein composition of the ER, Golgi complex, and endosomal membranes. This is accomplished by the recognition of sorting signals within the cytosolic tails of cargo proteins, such as the C-terminal di-lysine motif required for COPI-dependent Golgi to ER transport (Cosson and Letourneur, 1994; Letourneur et al., 1994). However, there is a paucity of information on other types of sorting signals potentially recognized by the heptameric COPI complex. Here we show that the WD40 repeat domains of α- and β'-COP surprisingly bind to polyUb with remarkable specificity for the linkage type and length of the Ub chain. A chain of at least three K63-linked Ubs is required for productive interaction with the WD40 β-propeller domains. Indeed, it is tempting to speculate that the twin propeller domains of COPI evolved in order to bind long chains of Ub that could wrap around the two propeller domains. Moreover, we clearly demonstrate the significance of the Ub interaction *in vivo*. Deletion of the ubiquitin-binding, N-terminal WD40 repeat domain of β'-COP disrupts endosome to TGN transport of Snc1, but this trafficking step can be restored when we replace the WD repeat domain with a 30-residue Tab2 NZF domain, which specifically binds K63-linked polyUb. By contrast, replacement of this β'-COP domain with a K48-linkage specific binding domain (Mud1 UBA domain) failed to restore Snc1 trafficking. Ub binding appears to be a conserved function for COPI as the human β'-COP N-terminal propeller also binds ubiquitin and functionally replaces its yeast counterpart in the Snc1 recycling pathway. Importantly, ubiquitin binding by β'-COP has no influence on COPI's role in Rer1 transport between the Golgi and ER, or the localization of Emp47. Therefore, we demonstrate a specific role for COPI at the early endosome that is independent of its function at the Golgi.

Exocytic v-SNARE recycling - may the circle be unbroken

The recycling of exocytic v-SNAREs is a multi-step process that begins with the fusion of these vesicles with the plasma membrane. The v- and t-SNAREs initially form a *trans*-SNARE complex that bridges the two bilayers and drives their fusion, which deposits the v-SNARE into the plasma membrane in a tight *cis*-SNARE complex (Weber et al., 1998). The AAA-ATPase

NSF/Sec18 catalyzes the separation of the *cis*-SNARE complexes at the plasma membrane freeing the v-SNARE for endocytosis (Grote et al., 2000; Miller et al., 2011). For Snc1 and related mammalian v-SNAREs (e.g. VAMP2), the clathrin adaptor proteins AP180 and CALM recognize conserved Val and Met residues within the SNARE motif, which prevents re-association with the t-SNAREs and promotes endocytosis into clathrin coated vesicles (Burston et al., 2009; Miller et al., 2011). These exocytic v-SNARE are not simply passive cargos in the subsequent steps as they mediate fusion of the endocytic vesicle with early endosomes (Antonin et al., 2000). Snc1 is ubiquitinated on Lys49, Lys63 and Lys75 within the SNARE motif (Swaney et al., 2013) and these modifications likely inactivate Snc1 and prevent re-association with the endosomal t-SNAREs (Tlg1, Tlg2 and Vti1) after dissociation by Sec18. Another relevant example is that monoubiquitination of Golgi SNAREs during mitosis is thought to inhibit their function as fusogens and facilitate Golgi fragmentation (Huang et al., 2016). The polyUb chains on Snc1 also form the sorting signal that allows efficient departure from early endosomes in COPI-coated vesicles. The ubiquitin signal appears to be a transient modification because only a small percentage of Snc1 is modified at steady-state, and it is likely that the ubiquitin is removed by an endogenous DUB to allow Snc1 to mediate fusion of recycling vesicles with the TGN.

Mechanistic insight into the role of COPI on early endosomes

COPI localizes primarily to early Golgi cisternae, although a portion of COPI also localizes to early endosomes in animal cells (Whitney et al., 1995) and we show here that this is also true in budding yeast. While mammalian cells deficient for a COPI subunit display trafficking defects in the endosomal system (Aniento et al., 1996; Tamayo et al., 2008; Whitney et al., 1995), it remains unclear if the endosomal trafficking defects are a direct effect of COPI depletion, or an indirect effect of perturbing the Golgi complex. No specific pathways or cargo sorting events mediated by endosomal COPI were known prior to this study. Furthermore, it was unclear how COPI would recognize a sorting signal on a membrane protein at the endosome, but ignore that signal as the cargo moved from the ER and through the Golgi to reach the endosome. We show here a direct and mechanistic role for the endosomal pool of COPI in a sorting ubiquitinated SNARE for return to the Golgi. By using a post-translational modification as the sorting signal, newly synthesized Snc1 can flow through secretory pathway without engaging COPI until it is ubiquitinated within

the endosomal system. Our discovery that COPI mediates EE to TGN delivery of a SNARE helps resolve a long-standing conundrum regarding the function of endosomal COPI.

The direct role of COPI in Snc1 recycling helps illuminate the potential functions of the other trafficking components in this pathway. COPI is recruited to membranes by the small GTP binding protein Arf, which is regulated by multiple ArfGEFs and ArfGAPs (Jackson and Casanova, 2000). We have previously shown that the ArfGAP Gcs1 is specifically recruited to the early endosome by its ability to sense the curvature and charge imparted to the membrane by the Drs2 phosphatidylserine flippase (Xu et al., 2013). Gcs1 also binds directly to Snc1 and to COPI (Robinson et al., 2006; Suckling et al., 2015), and these interactions likely stabilize the COPI-Ub interactions to productively recruit Snc1 into the COPI-coated vesicles. Deletion of *GCS1* has a modest influence on Snc1 recycling relative to β'-COP (Δ2-304) or *drs2*Δ (Xu et al., 2013) and so we expect there are other effectors of Drs2 acting in the pathway and that the COPI interaction with Ub-Snc1 is primarily responsible for the sorting reaction. The F-box protein Rcy1 binds directly to a regulatory domain in the C-terminus of Drs2 (Hanamatsu et al., 2014), and binding of an ArfGEF (Gea2) to this Drs2 regulatory domain stimulates phosphatidylserine flippase activity (Hsu et al., 2014; Natarajan et al., 2004). Thus, the function of Rcy1 in this pathway may be activation of Drs2. The relationship of the Snx4/41/42 complex to the COPI-Gcs1-Drs2-Rcy1 network is less clear, but a recent study suggests this sorting nexin complex may be localized to late endosomes and could represent a distinct pathway for retrieval of Snc1 (Ma et al., 2017). Further work will be needed to determine precisely how these components work together with COPI to drive Snc1 transport from EEs to the TGN.

In summary, our studies identify a new function for an old coat and define a specific trafficking function for COPI in the endosomal system. Further work is required to determine if mammalian exocytic SNAREs are recycled by this same mechanism and to identify other cargos that use a ubiquitin signal for sorting by COPI.

REFERENCES:

Aniento, F., F. Gu, R.G. Parton, and J. Gruenberg. 1996. An endosomal beta COP is involved in the pH-dependent formation of transport vesicles destined for late endosomes. *J Cell Biol*. 133:29-41.

Antonin, W., C. Holroyd, R. Tikkanen, S. Honing, and R. Jahn. 2000. The R-SNARE endobrevin/VAMP-8 mediates homotypic fusion of early endosomes and late endosomes. *Mol Biol Cell*. 11:3289-3298.

Burston, H.E., L. Maldonado-Baez, M. Davey, B. Montpetit, C. Schluter, B. Wendland, and E. Conibear. 2009. Regulators of yeast endocytosis identified by systematic quantitative analysis. *J Cell Biol*. 185:1097-1110.

Chen, S.H., A.H. Shah, and N. Segev. 2011. Ypt31/32 GTPases and their F-Box effector Rcy1 regulate ubiquitination of recycling proteins. *Cell Logist*. 1:21-31.

Cosson, P., and F. Letourneur. 1994. Coatomer interaction with di-lysine endoplasmic reticulum retention motifs. *Science*. 263:1629-1631.

Dodonova, S.O., P. Diestelkoetter-Bachert, A. von Appen, W.J. Hagen, R. Beck, M. Beck, F. Wieland, and J.A. Briggs. 2015. VESICULAR TRANSPORT. A structure of the COPI coat and the role of coat proteins in membrane vesicle assembly. *Science*. 349:195-198.

Eugster, A., G. Frigerio, M. Dale, and R. Duden. 2004. The alpha- and beta'-COP WD40 domains mediate cargo-selective interactions with distinct di-lysine motifs. *Mol Biol Cell*. 15:1011-1023.

Faini, M., R. Beck, F.T. Wieland, and J.A. Briggs. 2013. Vesicle coats: structure, function, and general principles of assembly. *Trends Cell Biol*. 23:279-288.

Fiedler, K., M. Veit, M.A. Stamnes, and J.E. Rothman. 1996. Bimodal interaction of coatomer with the p24 family of putative cargo receptors. *Science*. 273:1396-1399.

Galan, J.M., A. Wiederkehr, J.H. Seol, R. Haguenauer-Tsapis, R.J. Deshaies, H. Riezman, and M. Peter. 2001. Skp1p and the F-box protein Rcy1p form a non-SCF complex involved in recycling of the SNARE Snc1p in yeast. *Mol Cell Biol*. 21:3105-3117.

Gerst, J.E., L. Rodgers, M. Riggs, and M. Wigler. 1992. SNC1, a yeast homolog of the synaptic vesicle-associated membrane protein/synaptobrevin gene family: genetic interactions with the RAS and CAP genes. *Proc Natl Acad Sci U S A*. 89:4338-4342.

Grote, E., C.M. Carr, and P.J. Novick. 2000. Ordering the final events in yeast exocytosis. *J Cell Biol*. 151:439-452.

Hanamatsu, H., K. Fujimura-Kamada, T. Yamamoto, N. Furuta, and K. Tanaka. 2014. Interaction of the phospholipid flippase Drs2p with the F-box protein Rcy1p plays an important role in early endosome to trans-Golgi network vesicle transport in yeast. *J Biochem*. 155:51-62.

Hsu, J.W., Z.J. Chen, Y.W. Liu, and F.J. Lee. 2014. Mechanism of action of the flippase Drs2p in modulating GTP hydrolysis of Arl1p. *J Cell Sci*. 127:2615-2620.

Hua, Z., P. Fatheddin, and T.R. Graham. 2002. An essential subfamily of Drs2p-related P-type ATPases is required for protein trafficking between Golgi complex and endosomal/vacuolar system. *Mol Biol Cell*. 13:3162-3177.

Huang, S., D. Tang, and Y. Wang. 2016. Monoubiquitination of Syntaxin 5 Regulates Golgi Membrane Dynamics during the Cell Cycle. *Dev Cell*. 38:73-85.

Jackson, C.L., and J.E. Casanova. 2000. Turning on ARF: the Sec7 family of guanine-nucleotide-exchange factors. *Trends Cell Biol*. 10:60-67.

Jackson, L.P. 2014. Structure and mechanism of COPI vesicle biogenesis. *Curr Opin Cell Biol*. 29:67-73.

Jackson, L.P., M. Lewis, H.M. Kent, M.A. Edeling, P.R. Evans, R. Duden, and D.J. Owen. 2012. Molecular basis for recognition of dilysine trafficking motifs by COPI. *Dev Cell*. 23:1255-1262.

Komander, D., M.J. Clague, and S. Urbe. 2009. Breaking the chains: structure and function of the deubiquitinases. *Nat Rev Mol Cell Biol*. 10:550-563.

Letourneur, F., E.C. Gaynor, S. Hennecke, C. Demolliere, R. Duden, S.D. Emr, H. Riezman, and P. Cosson. 1994. Coatomer is essential for retrieval of dilysine-tagged proteins to the endoplasmic reticulum. *Cell*. 79:1199-1207.

Lewis, M.J., B.J. Nichols, C. Prescianotto-Baschong, H. Riezman, and H.R. Pelham. 2000. Specific retrieval of the exocytic SNARE Snc1p from early yeast endosomes. *Mol Biol Cell*. 11:23-38.

Ma, M., C.G. Burd, and R.J. Chi. 2017. Distinct complexes of yeast Snx4 family SNX-BARs mediate retrograde trafficking of Snc1 and Atg27. *Traffic*. 18:134-144.

MacDonald, C., J.A. Payne, M. Aboian, W. Smith, D.J. Katzmann, and R.C. Piper. 2015. A family of tetraspans organizes cargo for sorting into multivesicular bodies. *Dev Cell*. 33:328-342.

MacDonald, C., S. Winistorfer, R.M. Pope, M.E. Wright, and R.C. Piper. 2017. Enzyme reversal to explore the function of yeast E3 ubiquitin-ligases. *Traffic*.

MacGurn, J.A., P.C. Hsu, and S.D. Emr. 2012. Ubiquitin and membrane protein turnover: from cradle to grave. *Annu Rev Biochem*. 81:231-259.

Miller, S.E., D.A. Sahlender, S.C. Graham, S. Honing, M.S. Robinson, A.A. Peden, and D.J. Owen. 2011. The molecular basis for the endocytosis of small R-SNAREs by the clathrin adaptor CALM. *Cell*. 147:1118-1131.

Natarajan, P., J. Wang, Z. Hua, and T.R. Graham. 2004. Drs2p-coupled aminophospholipid translocase activity in yeast Golgi membranes and relationship to in vivo function. *Proc Natl Acad Sci U S A*. 101:10614-10619.

Pashkova, N., L. Gakhar, S.C. Winistorfer, L. Yu, S. Ramaswamy, and R.C. Piper. 2010. WD40 repeat propellers define a ubiquitin-binding domain that regulates turnover of F box proteins. *Mol Cell*. 40:433-443.

Peng, J., J.E. Elias, C.C. Thoreen, L.J. Licklider, and S.P. Gygi. 2003. Evaluation of multidimensional chromatography coupled with tandem mass spectrometry (LC/LC-MS/MS) for large-scale protein analysis: the yeast proteome. *J Proteome Res*. 2:43-50.

Rein, U., U. Andag, R. Duden, H.D. Schmitt, and A. Spang. 2002. ARF-GAP-mediated interaction between the ER-Golgi v-SNAREs and the COPI coat. *J Cell Biol*. 157:395-404.

Robinson, M., P.P. Poon, C. Schindler, L.E. Murray, R. Kama, G. Gabriely, R.A. Singer, A. Spang, G.C. Johnston, and J.E. Gerst. 2006. The Gcs1 Arf-GAP mediates Snc1,2 v-SNARE retrieval to the Golgi in yeast. *Mol Biol Cell*. 17:1845-1858.

Rothman, J.E. 1994. Mechanisms of intracellular protein transport. *Nature*. 372:55-63.

Sato, K., M. Sato, and A. Nakano. 2001. Rer1p, a retrieval receptor for endoplasmic reticulum membrane proteins, is dynamically localized to the Golgi apparatus by coatomer. *J Cell Biol*. 152:935-944.

Sato, Y., A. Yoshikawa, M. Yamashita, A. Yamagata, and S. Fukai. 2009. Structural basis for specific recognition of Lys 63-linked polyubiquitin chains by NZF domains of TAB2 and TAB3. *EMBO J*. 28:3903-3909.

Schroder-Kohne, S., F. Letourneur, and H. Riezman. 1998. Alpha-COP can discriminate between distinct, functional di-lysine signals in vitro and regulates access into retrograde transport. *J Cell Sci*. 111 (Pt 23):3459-3470.

Scott, C.C., F. Vacca, and J. Gruenberg. 2014. Endosome maturation, transport and functions. *Semin Cell Dev Biol*. 31:2-10.

Silva, G.M., D. Finley, and C. Vogel. 2015. K63 polyubiquitination is a new modulator of the oxidative stress response. *Nat Struct Mol Biol*. 22:116-123.

Stringer, D.K., and R.C. Piper. 2011. A single ubiquitin is sufficient for cargo protein entry into MVBs in the absence of ESCRT ubiquitination. *J Cell Biol*. 192:229-242.

Suckling, R.J., P.P. Poon, S.M. Travis, I.V. Majoul, F.M. Hughson, P.R. Evans, R. Duden, and D.J. Owen. 2015. Structural basis for the binding of tryptophan-based motifs by delta-COP. *Proc Natl Acad Sci U S A*. 112:14242-14247.

Sudhof, T.C., and J.E. Rothman. 2009. Membrane fusion: grappling with SNARE and SM proteins. *Science*. 323:474-477.

Swaney, D.L., P. Beltrao, L. Starita, A. Guo, J. Rush, S. Fields, N.J. Krogan, and J. Villen. 2013. Global analysis of phosphorylation and ubiquitylation cross-talk in protein degradation. *Nat Methods*. 10:676-682.

Tamayo, A.G., A. Bharti, C. Trujillo, R. Harrison, and J.R. Murphy. 2008. COPI coatomer complex proteins facilitate the translocation of anthrax lethal factor across vesicular membranes in vitro. *Proc Natl Acad Sci U S A*. 105:5254-5259.

Trempe, J.F., N.R. Brown, E.D. Lowe, C. Gordon, I.D. Campbell, M.E. Noble, and J.A. Endicott. 2005. Mechanism of Lys48-linked polyubiquitin chain recognition by the Mud1 UBA domain. *EMBO J*. 24:3178-3189.

Waters, M.G., T. Serafini, and J.E. Rothman. 1991. 'Coatomer': a cytosolic protein complex containing subunits of non-clathrin-coated Golgi transport vesicles. *Nature*. 349:248-251.

Weber, T., B.V. Zemelman, J.A. McNew, B. Westermann, M. Gmachl, F. Parlati, T.H. Sollner, and J.E. Rothman. 1998. SNAREpins: minimal machinery for membrane fusion. *Cell*. 92:759-772.

Whitney, J.A., M. Gomez, D. Sheff, T.E. Kreis, and I. Mellman. 1995. Cytoplasmic coat proteins involved in endosome function. *Cell*. 83:703-713.

Xu, P., R.D. Baldridge, R.J. Chi, C.G. Burd, and T.R. Graham. 2013. Phosphatidylserine flipping enhances membrane curvature and negative charge required for vesicular transport. *J Cell Biol*. 202:875-886.

Yip, C.K., and T. Walz. 2011. Molecular structure and flexibility of the yeast coatomer as revealed by electron microscopy. *J Mol Biol*. 408:825-831.

Zerial, M., and H. McBride. 2001. Rab proteins as membrane organizers. *Nat Rev Mol Cell Biol*. 2:107-117.

ACKNOWLEDGMENT:

We thank Scott Emr (Cornell University), Natalja Pashkova (University of Iowa), Richard Chi and Chris Burd (Yale University), Thomas Mund and Hugh Pelham (MRC) and Daniel Finley (Harvard Medical School) for plasmids and yeast strains. These studies were supported by NIH Grants 1R01GM118452 (to T.R.G.), 5R01GM058202 (to R.C.P.), 1R35GM119525 (to L.P.J.) and 1R01GM118491 (to J.A.M).

AUTHOR CONTRIBUTIONS:

P.X., J.A.M. L.P.J, R.C.P. and T.R.G. designed the study, P.X. performed the majority of the experiments and analyzed results, H.M.H. analyzed image data. R.C.P. and C.M. designed and performed the E3 ligase experiments. L.P.J and S.J.E. purified the WD40 repeat domains. R.C.P. designed and M.N.F. performed the NMR experiments. N.S.D. constructed some yeast strains. P.X. and T.R.G. wrote the paper implementing comments and edits from all authors.

Competing financial interests

The authors declare no other competing financial interests.

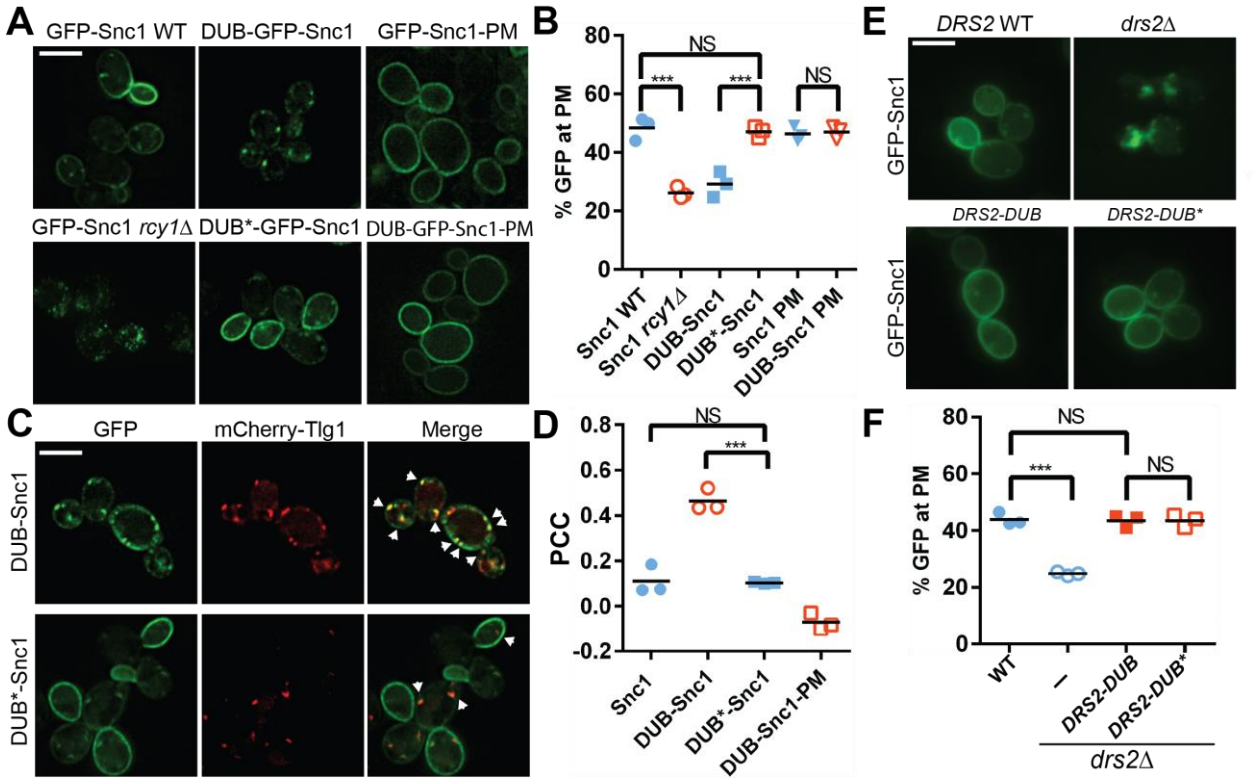

Figure 1. Ubiquitination is required for Snc1 recycling from early endosomes. (**A)** Fusion of catalytically active deubiquitinase (DUB), but not the inactive form (DUB*) to GFP-Snc1 blocks its recycling from endosomes comparably to *rcy1*Δ. Mutation of an endocytic signal (PM) in Snc1 prevents accumulation of DUB-GFP-Snc1-PM in cytosolic punctae. (**B)** Quantification of GFP intensity at the plasma membrane. At least 50 cells for three biological replicates of each genotype were analyzed, and the value and mean for each biological replicate was plotted. (**C)** DUB-GFP-Snc1 accumulates in early endosomes marked by mCherry-Tlg1. The arrowheads highlighted the punta showing colocalized GFP-Snc1 with mCherry-Tlg1. (**D**) Pearson correlation coefficient (PCC) GFP-Snc1 with mCherry-Tlg1. Each biological replicate plotted includes at least 20 cells. (**E**) Fusion of DUB to Drs2 does not disrupt the ability of Drs2 to support Snc1 recycling. (**F**) Quantification of GFP intensity at the plasma membrane for the cells in **(E).** Each biological replicate includes at least 50 cells. Statistical differences in (**B)**, (**D)** and (**E)** were determined using a one-way ANOVA on the means of three biological replicates (***, $P < 0.001$; NS, $P>0.05$). Scale bar in (**A)**, (**C)** and (**E)** represents 5µm.

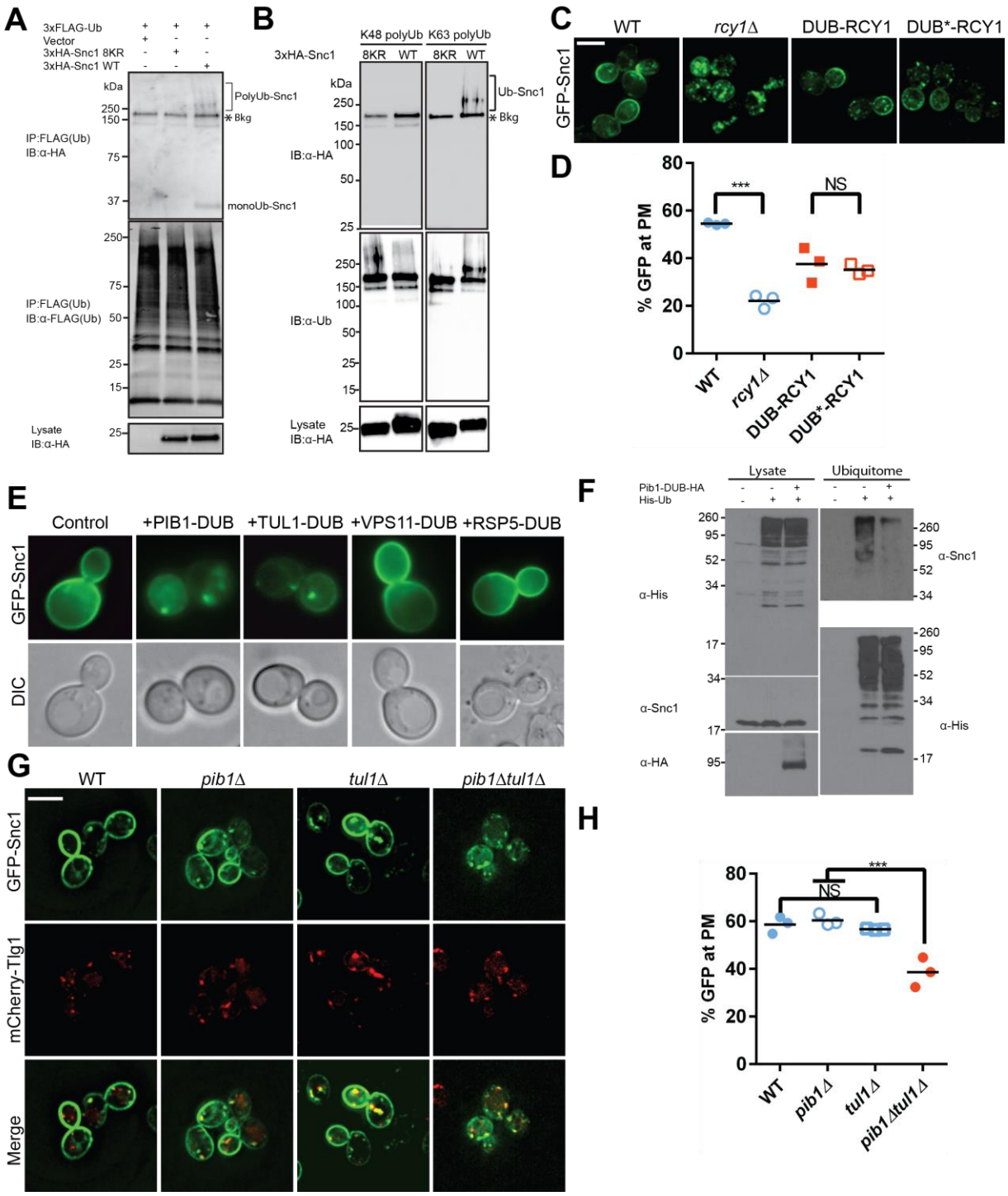

Figure 2. Snc1 is extensively modified with K63-linked polyUb chains. (**A**) Ubiquitinated proteins were immunoprecipitated from strains expressing 3X-FLAG-Ub and either an empty vector, a lysineless 3XHA-Snc1-8KR, or WT 3XHA-Snc1, and then immunobloted for HA-Snc1. Monoubiquitinated and polyubiquitinated Snc1 forms are indicated (based on predicted mobilities). The lysine-less 3XHA-Snc1-8KR is a specificity control and the asterisk indicate background bands. (**B**) Polyubiquitinated 3xHA-Snc1 is recovered in anti-K63 TUBE precipitated

samples from cell lysates, but not anti-K48 TUBE precipitates. One of three experimental replicates is shown. (**C**) Rcy1 appears to play a role in Snc1 recycling that is independent of Ub ligase activity. A fusion of DUB or DUB* to the amino terminus of Rcy1 caused a partial defect in Snc1 recycling when expressed in *rcy1*Δ cells (BY4742 YJL204C). However, there was no significant difference between DUB and DUB*, indicating that the effect of the DUB is unrelated to its deubiquitinase activity. (**D**) Quantification of GFP intensity at the plasma membrane. (**E**) WT cells (BY4742) overexpressing GFP-Snc1 and DUB fusions with several candidate E3 Ub ligases. PIB1-DUB and TUL1-DUB were the only ligase-DUB fusions that caused a GFP-Snc1 recycling defect. (**F**) DUB tagged Pib1 significantly reduced endogenous polyubiquitinated Snc1. Ubiquitinated proteins (Ubiquitome) were recovered from cells expressing His-tagged Ub with or without Pib1-DUB and probed for endogenous, untagged Snc1 and His-Ub. Much less polyubiquitinated Snc1 was recovered from the ubiquitome in cells expressing DUB-Pib1. DUB-Pib1-HA expression was confirmed by immunoblot with anti-HA antibody. (**G**) The *pib1*Δ (PLY5293) and *tul1*Δ (PLY5294) single mutants recycled GFP-Snc1 normally, but the *pib1*Δ *tul1*Δ (PXY64) double mutant displayed a recycling defect. (**H**) Quantification of GFP intensity at the plasma membrane for cells shown in **(G)**. Each biological replicate includes at least 50 cells for data plotted in (**D**) and (**H**). Statistical differences were determined using a one-way ANOVA on the means of three biological replicates. (***, $P < 0.001$; NS, $P>0.05$). Scale bar in (**C**) and (**G**) represents 5µm.

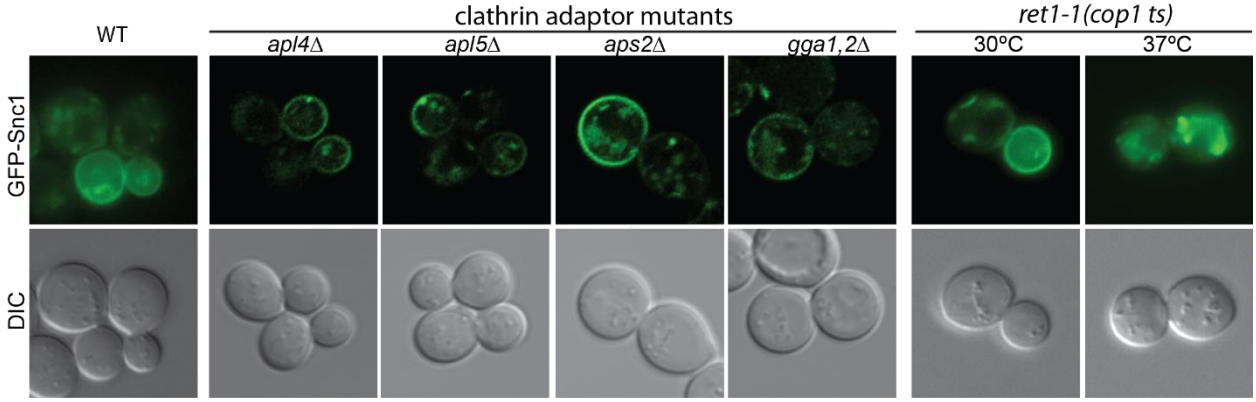

Figure 2-figure supplement 1. Inactivation of a COPI temperature-sensitive allele (*ret1-1*) at the non-permissive temperature (37°C) blocked GFP-Snc1 recycling. By contract, GFP-Snc1 still could localize to the plasma membrane in the clathrin adaptor AP1 (*apl4*Δ), AP3 (*apl5Δ*), AP2 (*aps2Δ*) or GGA (*gga1,2Δ)* mutants.

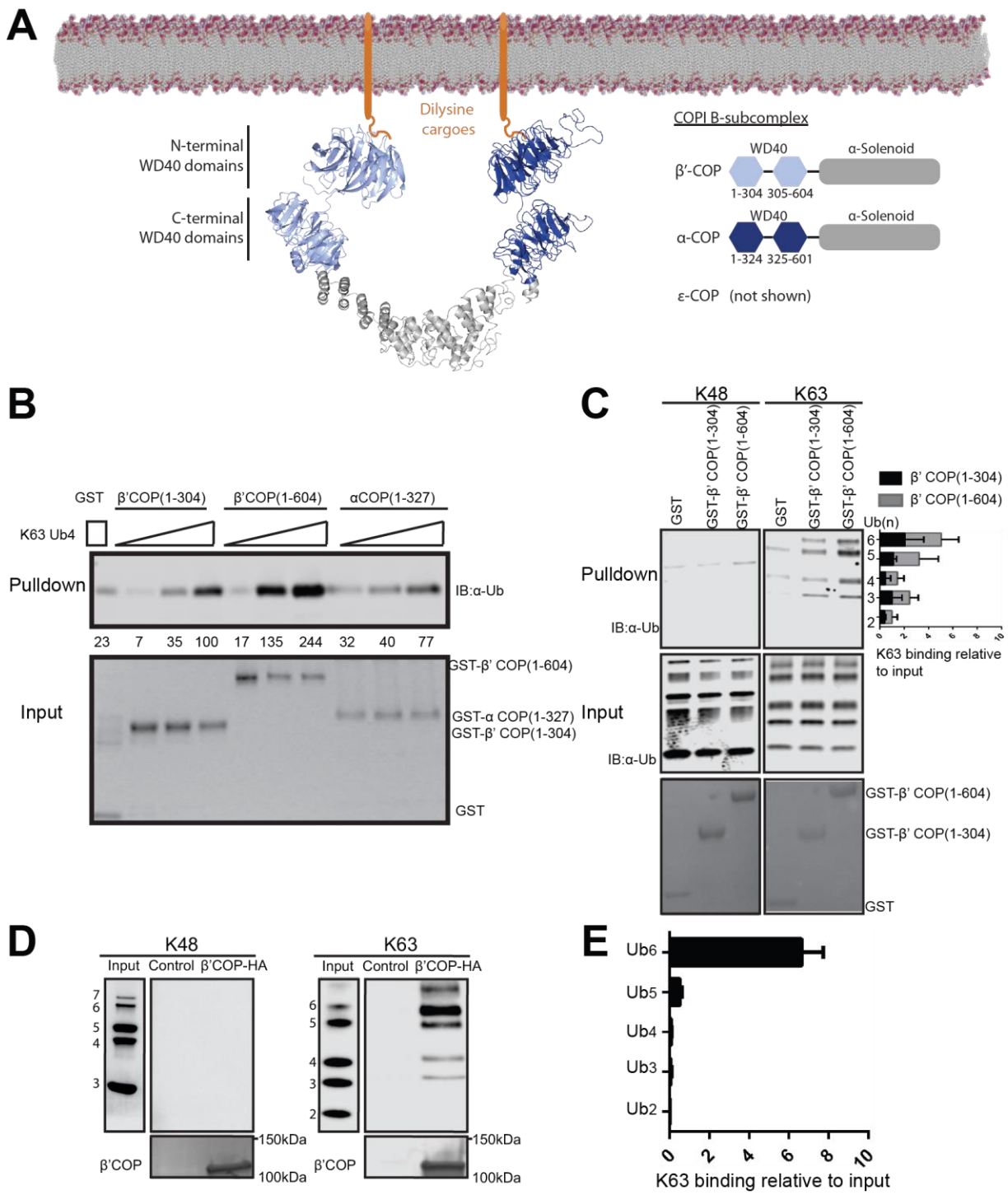

Figure 3. WD40 repeat propeller domains of COPI bind K63-linked polyubiquitin. (**A**) Structures of α- and β'-COP from the COPI B-subcomplex shown binding dilysine cargo in the membrane. **(B)** GST-β' COP (1-604), GST-β' COP (1-304) and GST-α COP (1-327) bind K63-linked tetraUb relative to the GST only control. 0.5μM of GST and GST tagged WD40 proteins immobilized glutathione beads were incubated 125nM, 250nM or 500nM of K63-Ub_4. Values are tetraUb band intensities from this experiment. (**C**) Both GST-β' COP (1-604) and GST-β' COP (1-304) preferentially binds long K63-linked chains of Ub. Quantification of K63 binding relative to input

(100*(band signal intensity – corresponding GST lane)/ input band intensity). The values represent mean ± SEM from three independent binding experiments. (**D**) COPI isolated from yeast on anti-HA beads also preferentially binds long K63-linked polyUb, but not K48-linked Ub. (**E**) Quantification of K63-linked Ub polymers binding relative to input. The values represent mean ± SEM from three independent binding experiments (100*band signal intensity/input band intensity).

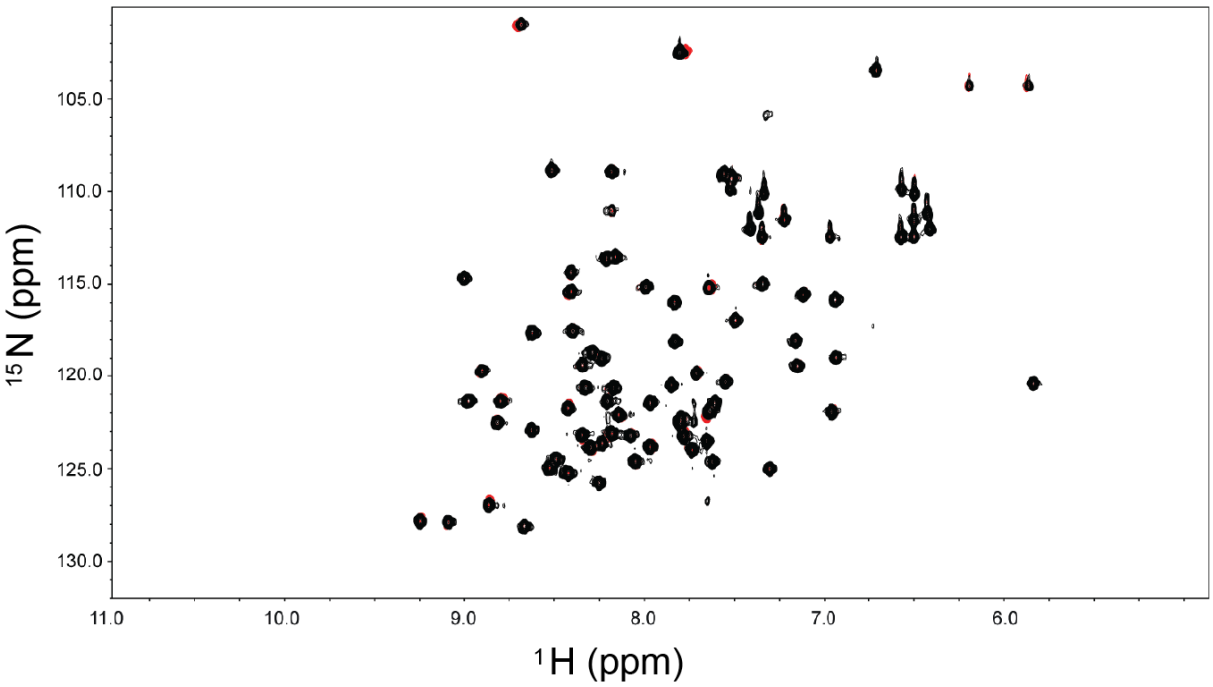

Figure 3-figure supplement 1. The N-terminal propeller of β'-COP (1-304) does not bind significantly to monoUb. HSQC spectra of 125μM ^{15}N-labeled ubiquitin in 40 mM $NaPO_4$ (pH=7.1) in the absence and presence of 1.25 mM unlabeled N-terminal propeller of β'COP. Spectra show an almost complete overlay of ^{15}N Ub alone (red) and in the presence of a 10-fold excess of the N-terminal propeller of β'COP (black).

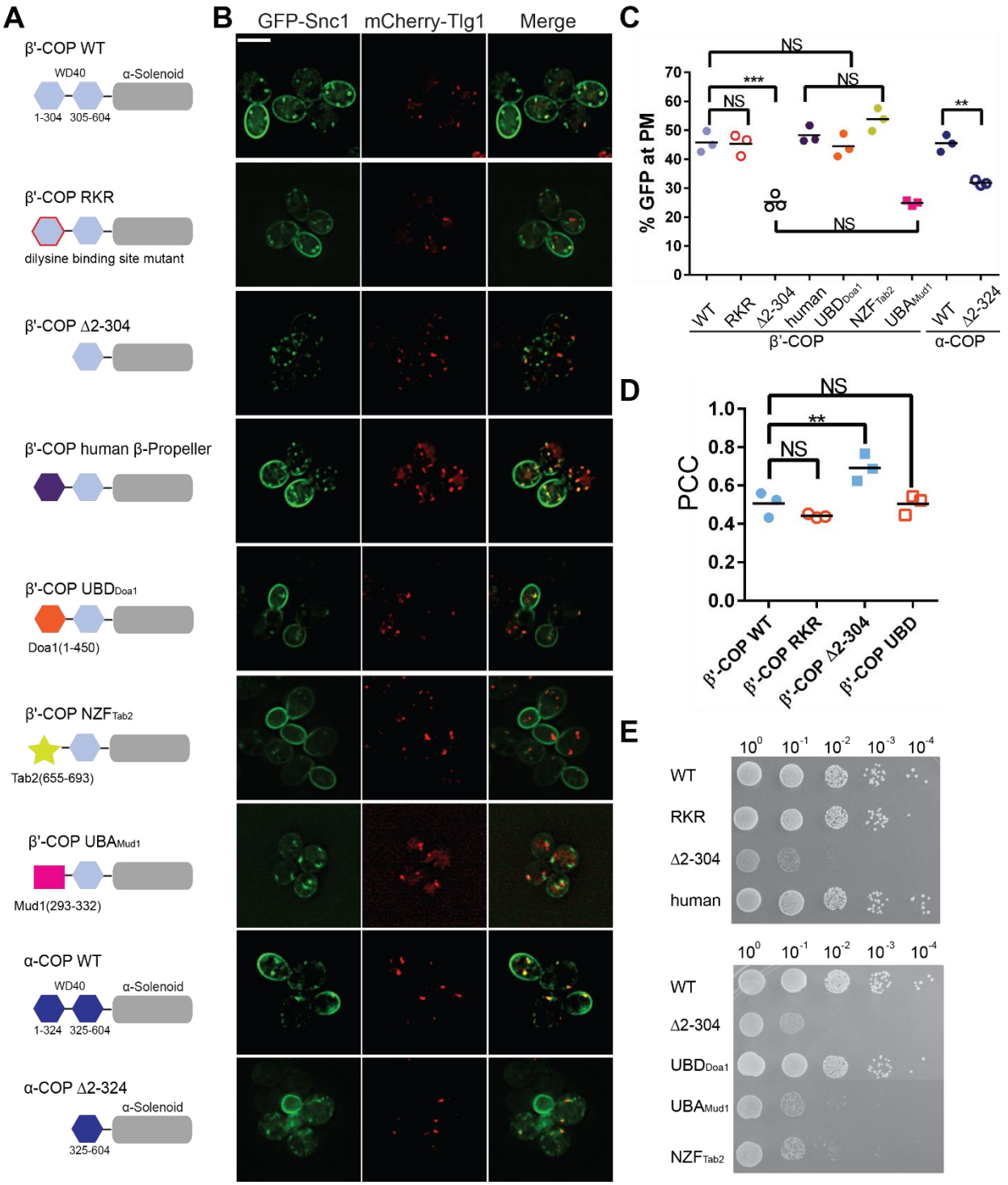

Figure 4. Ub binding by β'COP is required to sort GFP-Snc1 from early endosomes to the Golgi. (**A** and **B)** Deletion of the N-terminal WD40 propeller from β'COP (Δ2-304) disrupts recycling of GFP-Snc1 but mutation of residues within this propeller required for dilysine motif binding (RKR) have no effect. Replacement of the N-terminal propeller with a linkage independent ubiquitin-binding domain (UBD) from Doa1, a K63-specific Npl4 Zinc Finger (NZF) domain from Tab2, or the N-terminal propeller from human β'COP restored Snc1 recycling. In contrast, the K48-linkage specific ubiquitin pathway associated (UBA) domain from Mud1 failed to restore GFP-

Snc1 recycling. Deletion of N-terminal WD40 propeller of α-COP caused a partial Snc1 recycling defect. Scale bar, 5μm. (**C**) Quantification of GFP intensity at the plasma membrane. Each biological replicate includes at least 50 cells and individual biological replicates value and mean are shown. Statistical differences were determined using a one-way ANOVA on the means of the three biological replicates (***, $P < 0.001$; NS, $P>0.05$). (**D**) Quantification analysis of colocalization between GFP-Snc1 and mCherry-Tlg1 in WT and β'-COP mutant cells using Pearson correlation coefficient. Each replicate includes at least 20 cells and individual biological replicates value and mean were shown. **(E)** Serial dilution growth assay of β'COP mutants. The β'-COP dilysine motif binding mutant (RKR) had no effect on growth, but deletion of the first propeller (Δ2-304) caused slow growth. Replacement of the first propeller with the UBD or the human N-terminal propeller, but not NZF or UBA domains, restored WT growth. One of four replicates is shown.

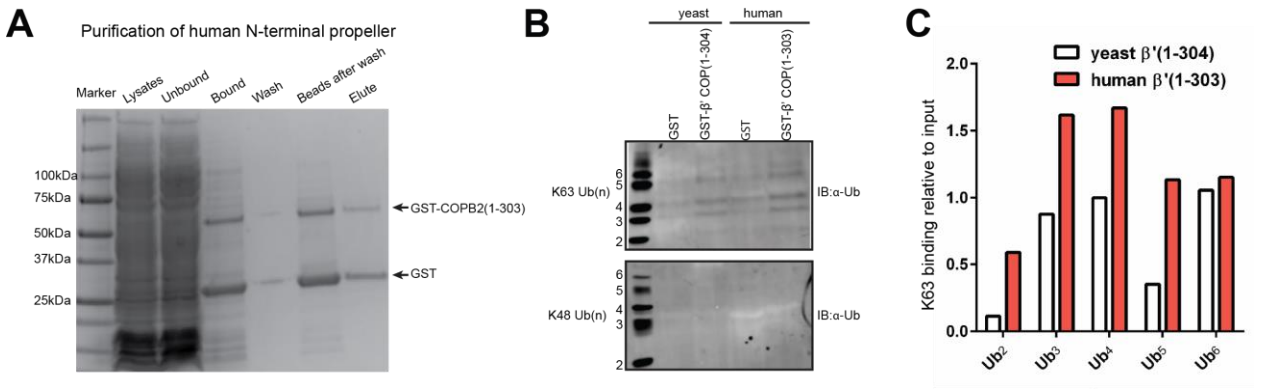

Figure 4-figure supplement 1A-C. Comparably to the yeast N-terminal propeller, the human N-terminal propeller also preferentially binds K63-linked ubiquitin chains. (**a**) The GST-tagged human N-terminal propeller of COPB2(1-303) purified as described for the yeast. Note there is GST expression as well. (**b**) Equal molar concentrations of GST alone, or GST-tagged yeast or human N-terminal propeller domains proteins were incubated with K63-linked and K48-linked polyubiquitin chain mixtures. The amounts bound were detected by immunoblot using anti-Ub antibody. (**c**) The percentage of the band intensity divided by the input band intensity was taken as the relative binding. The value represents the average relative binding from two independent binding assays.

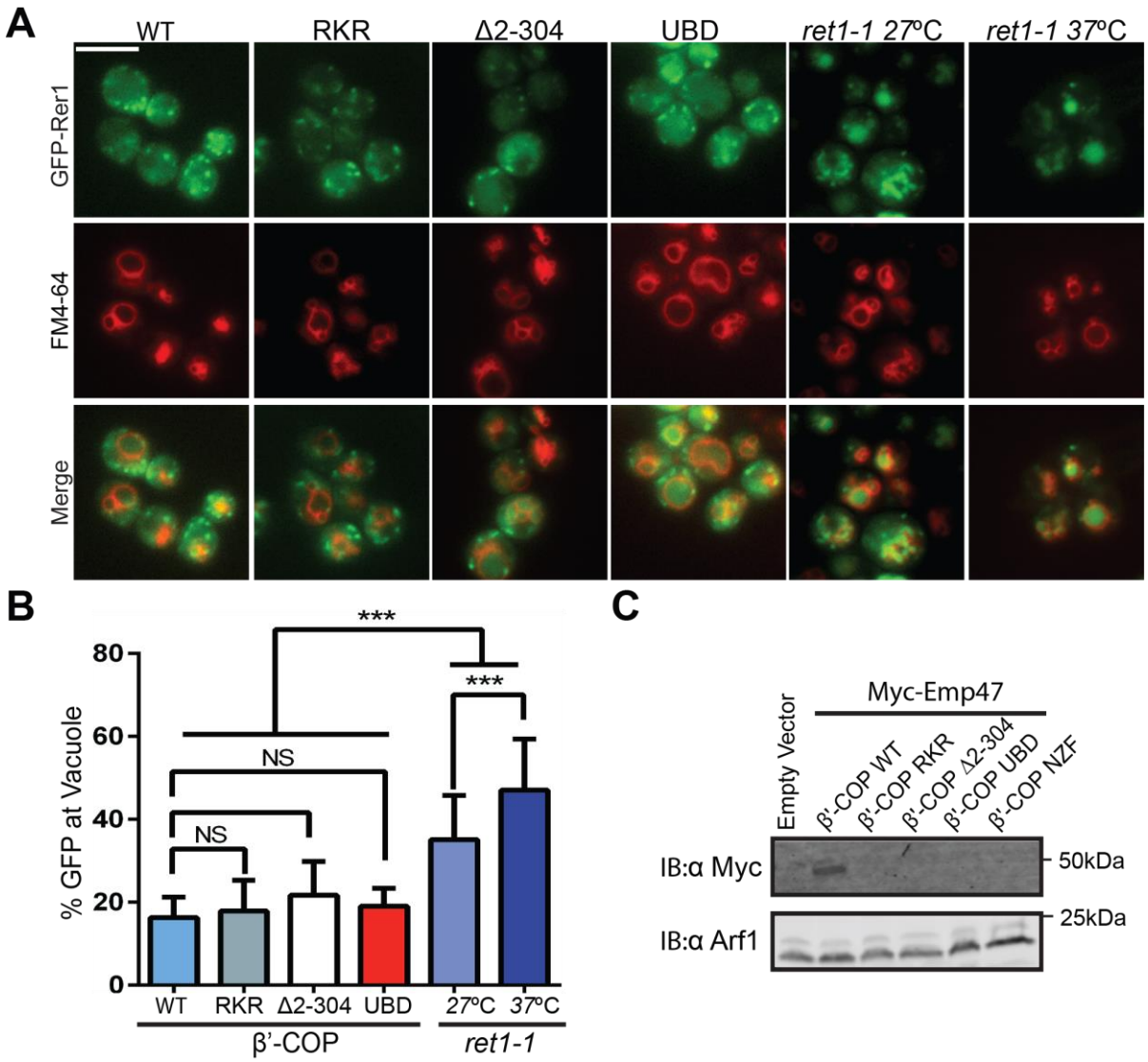

Figure 5 β'-COP interaction with ubiquitin has no role in the COPI-dependent trafficking of Rer1 or Emp47 at the Golgi complex. (**A**) Deletion of N-terminal WD40 propeller of β'-COP does not alter the retrograde trafficking of Rer1 from cis-Golgi to endoplasmic reticulum. The indicated β' COP mutant cells expressing GFP-Rer1 were labeled with 2nM FM4-64 for 20 minutes at 30˚C then chased for 2 hours to label vacuole membranes. An α-COP temperature-sensitive mutant (*ret1-1*) expressing GFP-Rer1 was labeled with 2nM FM4-64 at 27˚C for 20 minutes, then chased at 27˚C or 37˚C for 2 hours. (**B**) Quantification of GFP-Rer1 in the vacuole. At least 20 cells were used to calculate the percentage of GFP intensity in the vacuole. Values represent mean ± SD. Statistical differences were determined using a one-way ANOVA on the means of three biological replicates. (***, $P < 0.001$; NS, $P>0.05$). (**C**) Immunoblot showing that Myc-Emp47, an early Golgi COPI cargo, is missorted into the vacuole and degraded in strains expressing β'COP RKR or Δ2-304, but stability is not restored when the N-terminal propeller is replaced with Ub binding domains. Immunoblot using anti-Arf1 is used as the loading control.

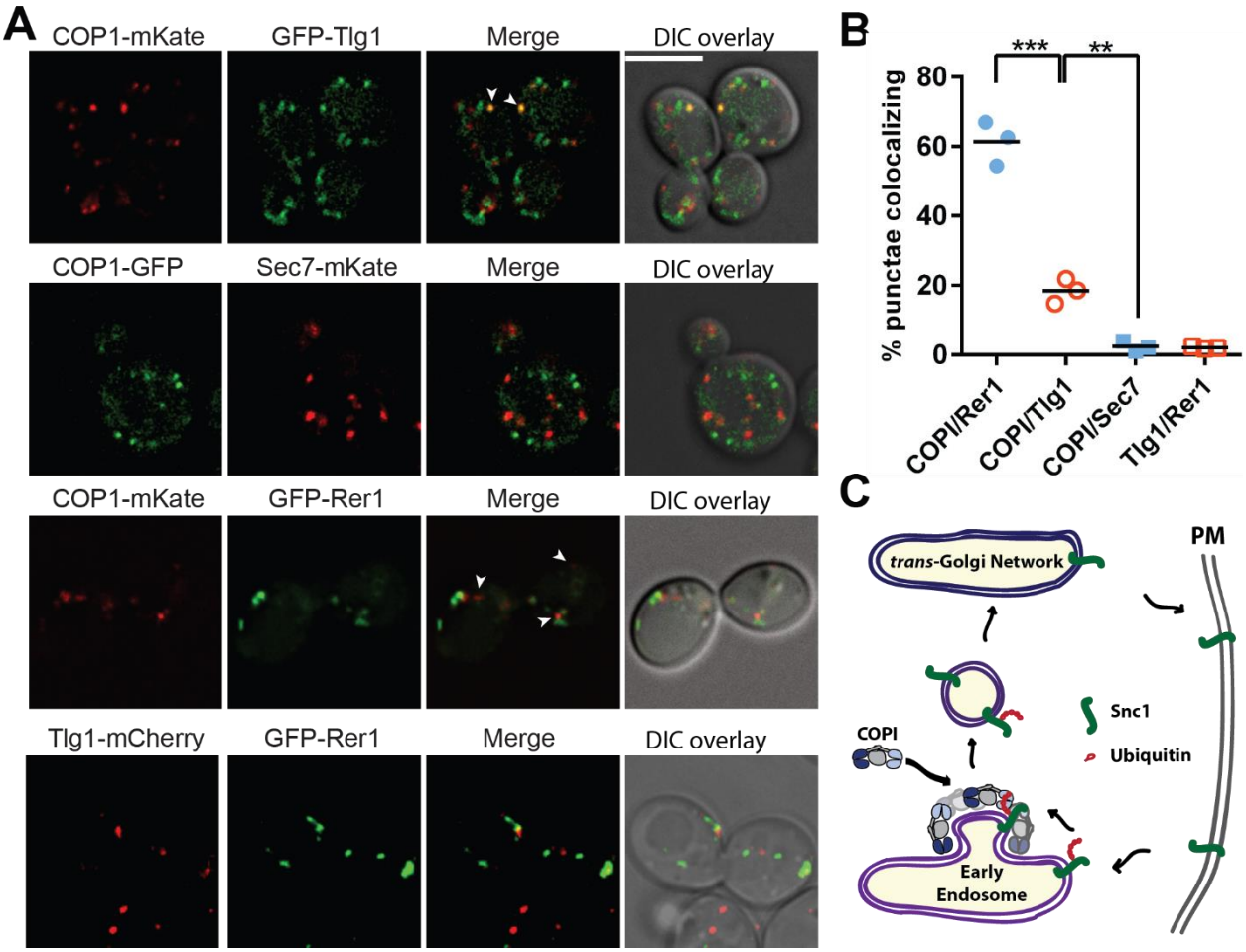

Figure 6. A small pool of COPI localizes to early endosomes in yeast. (**A** and **B**) Co-localization of Cop1 (α-COP) with markers for the early endosome/TGN (Tlg1), early Golgi (Rer1), or TGN (Sec7). Tlg1 was also co-localized relative to Rer1 to make sure there was no significant overlap between these early Golgi and early endosome markers. Scale bar, 5μm. Statistical differences were determined using a one-way ANOVA on the means of three biological replicates (***, $P < 0.001$; **, $P<0.01$; NS, $P>0.05$). (**C**) Proposed function of COPI at early endosomes is to directly bind K63-linked polyubiquitin chains on Snc1 and package this cargo into COPI-coated vesicles targeted to the *trans*-Golgi net.

METHOD

Reagents.

EZview Red ANTI-FLAG M2 Affinity Gel (F2426), 3xFLAG Peptide (F4799), Glutathione−Agarose (G4510), N-Ethylmaleimide (S1638), Iodoacetamide (GERPN6302), aprotinin (A1153), pepstatin (P5318) and Phenylmethanesulfonyl fluoride (P7626) were purchased from Sigma-Aldrich (St Louis, MO). K11-, K48-, and K63-linked poly-ubiquitin chains (Ub2-7) were purchased from Boston Biochem (Cambridge, MA) and K63-linked tetra-ubiquitin was purchased from UBPBio (Aurora, CO). Protease inhibitor tablet (PI88665), Coomassie Brilliant Blue R-250 Dye (20278), and FM4-64 dye (T-3166) were purchased from ThermoFisher Scientific (San Jose, CA). ECL Prime Western Blotting Detection Reagent (RPN2236) was purchased from GE healthcare Life Sciences (Marlborough, MA). Anti-K63 TUBE1 (UM604) and anti-K48 TUBE (UM605) were purchased from LifeSensors (Malvern, PA).

Antibodies.

The rabbit anti-Arf1 (1:10,000) and rabbit anti-Drs2 (1:2000) antibodies have been described previously (Chen et al., 1999). Mouse anti-GFP (1C9A5, 1:2000) and mouse anti-Myc (9E10, 1:2000) antibodies were purchased from the Vanderbilt Antibody and Protein Repository (Nashville, TN). Mouse anti-FLAG M2 (F1804, 1:2000) and mouse anti-HA (12CA5, 1:5000) were purchased from Sigma-Aldrich. Mouse anti-Ubiquitin antibody (MAB1510, 1:1000) was purchased from EMD Millipore (Billerica, MA). All secondary antibodies, including IRDye® 680LT Goat anti-Mouse (1:20,000), IRDye® 800CW Goat anti-Mouse (1:20,000), and IRDye® 680LT Goat anti-Rabbit (1:20,000), were purchased from LI-COR Biosciences (Lincoln, NE).

Strains and plasmids.

Standard media and techniques for growing and transforming yeast were used. Epitope tagging of yeast genes was performed using a PCR toolbox (Janke et al., 2004). COPI mutant strains were constructed by plasmid shuffling (PXY51) on 5'-fluoro-orotic acid (5-FOA) plates. Plasmid constructions were performed using standard molecular manipulation. Mutations were introduced using a Q5® Site-Directed Mutagenesis Kit or Gibson Assembly® Master Mix (NEW ENGLAND BioLab). Supplementary Table 1. List of plasmids used in this study; Supplementary Table 2. List of yeast strains used in this study.

DUB comes from herpes simplex virus UL36 and DUB* was constructed by point mutation C56S and deletion of ubiquitin binding β-hairpin (130-147) on DUB.

Imaging and image analysis.

To visualize GFP- or mCherry-tagged proteins, cells were grown to early-to-mid-logarithmic phase, harvested, and resuspended in imaging buffer (10 mM Na_2PHO4, 156 mM NaCl, 2 mM KH_2PO4, and 2% glucose). Cells were then mounted on glass slides and observed immediately at room temperature. Most

749 images were acquired using a DeltaVision Elite Imaging system equipped with a 63× objective lens
750 followed by deconvolution using SoftWoRx software (GE Healthcare Life Science). All other images were
751 acquired using an Axioplan microscope (Carl Zeiss) equipped with a 63× objective lens with an sCMOS
752 camera (Zyla ANDOR) and Micro-Manager software. Overlay images were created using the merge
753 channels function of ImageJ software (National Institutes of Health). GFP-Snc1 at the plasma membrane is
754 quantified as previously described (Hankins et al., 2015). Briefly, concentric circles were drawn just inside
755 and outside the plasma membrane using Image J to quantify the internal fluorescence and total fluorescence,
756 respectively. The internal fluorescence was subtracted from the total to give the GFP intensity at the plasma
757 membrane. At least 50 randomly chosen cells from three biological replicates (independently isolated
758 strains with the same genotype) were used to calculate the mean and standard deviation. To quantify GFP-
759 Snc1 colocalization with Tlg1, a Pearson's Correlation Coefficient (PCC) for the two markers in each cell
760 (n =3, 20 cells each) was calculated using the ImageJ plugin Just Another Colocalization Plugin with Costes
761 Automatic Thresholding (Bolte and Cordelieres, 2006). The percentage of COPI colocalization with the
762 different organelle markers was calculated by counting how many COPI puncta (n=3, >100 puncta each)
763 colocalized with the markers.

764 **Purified recombinant proteins.**

765 GST-tagged recombinant proteins were expressed and purified as previously described (Jackson et al.,
766 2012). Briefly, BL21(DE3)-pLysS (Agilent Technologies) *Escherichia coli* cells containing plasmids
767 encoding each fusion protein were grown in 6 L of YT medium (16g Tryptone, 10g Yeast Extract and 5g
768 NaCl) containing 100 mg/ml ampicillin at 240 rpm at 37°C to an OD600 of 0.8. The expression was induced
769 with 0.2 mM IPTG overnight at 22°C. Cells were harvested by centrifugation at 5,000 g for 10 min and
770 stored at −80°C. Cells expressing β'-COP constructs were lysed in 20 mM Tris,pH 7.4, 200 mM NaCl, 2
771 mM DTT, 2 µg/µl aprotinin, 0.7 µg/ml pepstatin. α-COP GST fusion proteins were purified in 20 mM Tris,
772 pH 7.4, 500 mM NaCl, 2 mM DTT, 2 µg/µl aprotinin, 0.7 µg/ml pepstatin. Cells were lysed by a disruptor
773 (Constant Systems Limited, Daventry, UK), and the lysates were centrifuged at 30,000 rpm for 1 hour. The
774 supernatant was incubated with 5ml of glutathione-agarose beads 1 hour at 4°C. The beads were washed in
775 a column with 200ml of washing buffer (20 mM Tris-HCl and 200 mM NaCl, pH 7.5), then eluted in 1 ml
776 fractions with GST elution buffer (50 mM Tris-HCl and 20 mM reduced glutathione, pH 9.5). The protein
777 was equilibrated to neutral buffer (20 mM Tris-HCl and 100 mM NaCl, pH 6.8) using dialysis. All proteins
778 were further purified by gel filtration on a Superdex S200 preparative or analytical column (GE Healthcare).
779 Protein concentrations were measured by BCA assay (Sigma-Aldrich).

780 ***In vitro* binding assays.**

781 GST recombinant proteins were incubated with glutathione agarose beads in PBS at 25°C for 30 min. GST
782 fusions on beads were then incubated with 10x molecular amount of Ub_4 at 25°C for 1 hr in incubation

buffer (10 mM Na_2PHO4, 156 mM NaCl, 2 mM KH_2PO4, 0.1mg/ml BSA, and 0.01% Triton-X 100). Beads were then washed three times with wash buffer (10 mM Na_2PHO4, 156 mM NaCl, 2 mM KH_2PO4, and 0.01% Triton) and eluted with 50 µl Glutathione in PBS on ice for 10 min. The elution was then mixed with SDS-Urea sample buffer at 60°C for 10 minutes.

For the ubiquitin chain binding, 0.5µM of GST or GST tagged β-Prop was incubated with 9µg of ubiquitin chains in binding buffer (20 mM HEPES pH 7.5, 100 mM NaCl, 20 % Glycerol, 0.1 % NP-40, 200 µg/ml BSA) at 4°C overnight. The GST beads were then added for 30 minutes. After 3 washes, the bound proteins were eluted with SDS-Urea sample buffer at 60°C for 10 minutes (Sobhian et al., 2007). The protein samples were analyzed by SDS–PAGE followed by immunoblotting using primary antibody and IRDye® 680LT Goat anti-Mouse (1: 20,000). The membrane was imaged with Licor Odyssey CLx (Licor). The band intensities were quantified by Image Studio (Version 5.2). The relative binding was calculated as 100*(band signal intensity – corresponding GST lane)/ input band intensity.

NMR titration experiments.

Uniformly enriched ^{15}N-labeled ubiquitin prepared in 50 mM sodium phosphate pH 7.0, 1 mM DTT was diluted to 30 µM with 10% (v/v) D_2O. A sample of ^{15}N-labeled ubiquitin with 10:1 molar excess of β'-COP residues 1-304 was prepared in the same way. Standard two-dimensional ^{15}N-^{1}H HSQC spectra were collected at 25˚C on an 800 MHz Bruker Avance III spectrometer with a TCI triple resonance cryoprobe (Bruker BioSpin). Data were processed in Topspin 3.2 (Bruker BioSpin), with zero filling in the indirect dimension and squared sine bell apodization in both dimensions.

Construction of HA tagged β'-COP.

β'-COP was C-terminally tagged with 6xHA by integration of a PCR product amplified from pYM15 into the *SEC27* locus (Janke et al., 2004). Properly integrated clones were confirmed by genotyping PCR and immunoblot using anti-HA antibody.

Purification of yeast coatomer for *in vitro* Ub binding assays.

Affinity isolation of COPI was performed as previously described (Yip and Walz, 2011) with the following modifications. 2 L of wild type (BY4742) and C-terminal tagged 6xHA β'-COP (PXY57) yeast cells grown in YPD were pelleted when the OD600 reached ~4. After washing with cold water, the pellets were frozen. 5,000 OD of cells were resuspended in lysis buffer (10 mM Tris pH 7.4, 150 mM NaCl, 0.1% NP40, 2 mM EDTA, 50 mM NaF, 0.1 mM Na_3VO_4, 10 mM β-mercaptoethanol, 1 mM PMSF, and complete protease inhibitor tablet). Cells were broken using a Disruptor Genie (Scientific Industries) at 4°C for 10 min at 3000 setting with 0.5 mm diameter of glass beads. The lysates were centrifuged at 13,000 rpm for 20 min at 4°C and the supernatant was incubated with anti-HA agarose beads for 1 hour at 4°C. The anti-HA agarose beads were washed with 1 ml of lysis buffer three times.

Yeast coatomer binding assay.

The anti-HA beads with bound coatomer were incubated with 4µg of ubiquitin ladder mixtures in 500µl of binding buffer (20 mM HEPES pH 7.5, 100 mM NaCl, 20 % Glycerol, 0.1 % NP-40, 200 µg/ml BSA) at 4°C for 2 hours. After the beads were washed three times, the specifically bound polyubiquitin was eluted from the beads by 3xHA peptide (100µg/ml). The eluate was added to SDS-Urea sample buffer and heated at 60°C for 10 minutes. The protein samples were analyzed by SDS–PAGE followed by immunoblotting using primary anti-Ub antibody and anti–mouse IgG-HRP (1: 50,000 in TBST+5% non-fat milk). The membrane was developed by enhanced chemiluminescence (Amersham) and imaged with LAS 4000 ImageQuant (GE Healthcare Life Sciences). The band intensity was quantified by ImageQuant TL (GE Life Sciences). The relative binding was calculated as 100* (pulldown band intensity/the input band intensity).

Enrichment of ubiquitinated proteins by Anti-FLAG immunoprecipitation.

Immunoprecipitation was performed as described previously (Stringer and Piper, 2011) with the following modifications. 50 OD of cells at mid-log phage were pelleted and resuspended in 0.2 M NaOH for 2 min. The cells were pelleted and resuspended in Urea-SDS buffer (50 mM Tris, pH 6.8, 8 M urea, 5% SDS, 10% glycerol, 10mM N-ethylmaleimide, and 10mM iodoacetamide) and boiled at 70°C for 10 min. The cell lysates were diluted with 10 volumes of 0.1 M Tris, pH 7.5, 0.4% Triton X-100, 10mM N-ethylmaleimide and 10mM iodoacetamide and placed on ice for 10 min. After centrifugation at 13,000 rpm for 30 min, the supernatant was incubated with anti-FLAG agarose beads overnight. Beads were washed three times in 0.1 M Tris, pH 7.5, 0.4% Triton X-100. Anti-FLAG beads were eluted with 20µl 3xFLAG peptide (150 ng/µl in PBS) at 4°C for 30 min. The Supernatant mixed with 2x SDS-Urea sample buffer (40 mM Tris-HCl, pH 6.8, 8 M urea, 0.1 mM EDTA, 1% β-mercaptoethanol, and 5% SDS) was heated at 70°C for 10 min. The samples were then separated by 4-20% gradient SDS-PAGE followed by immunoblotting using the manufacturer's protocol (LI-COR Biosciences). PVDF membranes were scanned by an Odyssey CLx scanner and quantified using Image Studio™ Software (LI-COR Biosciences). To detect ubiquitinated proteins from yeast, the PVDF membrane was incubated anti-FLAG antibody (1:2500) followed by the incubation with anti-mouse IgG-HRP (1: 50,000 in TBST+5% non-fat milk) for 1 h at room temperature. After three washes in TBST, membranes were incubated with enhanced chemiluminescence (Amersham). The membrane was imaged with LAS 4000 ImageQuant.

Enrichment of K63 and K48-polyubiqutinated proteins.

The manufacturer's (LifeSensors) protocol was followed with the following modification (Silva et al., 2015). 50 OD of yeast cells collected at the mid-log growth phage were resuspended in lysis buffer (100 mM Tris pH 8.0, 150 mM NaCl, 5mM EDTA, 1% NP-40, 0.5% Triton-X 100, 5 mM NEM, complete protease inhibitor tablet). Cells were broken using a Disruptor Genie (Scientific Industries) at 4°C for 10 min at 3000 setting with 0.5 mm diameter glass beads. The lysates were centrifuged at 13,000 rpm for 20

min at 4°C and the clarified lysates were diluted with an 10-fold volume of buffer (100 mM Tris pH 8.0, 150 mM NaCl, 5mM EDTA) containing the same concentrations of protein inhibitors and NEM. A small portion of lysates was taken as the Input. Then the lysate was incubated with 100µM of FLAG anti-K63 TUBE1 or FLAG anti-K48 TUBE for 2 hours before incubating with FLAG M2 Affinity Resin overnight at 4°C. The beads were washed three times with washing buffer (100 mM Tris pH 8.0, 150 mM NaCl, 5mM EDTA, 0.05% NP-40). Finally, the polyubiquitinated proteins were eluted with 3xFLAG peptide (150 ng/µl in PBS), subjected to SDS-PAGE, and immunoblotted with anti-Ub or anti-HA as described above.

Quantification of GFP-Rer1 in the vacuole.

To label the vacuole of yeast cells, the cells expressing GFP-Rer1 were pulsed with 2nM of FM4-64 at 30°C for 20 minutes. Then the cells were chased in YPD for 2 hours (Vida and Emr, 1995) before the images were acquired using an Axioplan microscope (Carl Zeiss) equipped with a 63× objective lens with an sCMOS camera (Zyla ANDOR) and Micro-Manager software. Overlay images were created using the merge channels function of ImageJ software (National Institutes of Health). In ImageJ, the vacuole of a cell stained with FM4-64 was selected using the freehand draw tool and the same area was copied into the green (GFP) channel. The whole cell area was also defined using the freehand draw tool and the GFP in the vacuole is defined as $\text{Intensity}_{\text{vacuole}}$ / $\text{Intensity}_{\text{whole cell}}$. 20 cells were selected and quantified +/- SD.

Statistical analysis.

Statistical differences were determined using a one-way ANOVA on the means of at least three independent experiments using GraphPad Prism (GraphPad Software Inc.). Probability values of less than 0.05, 0.01 and 0.001 were used to show statistically significant differences and are represented with *, ** or *** respectively.

881 **Tables S1** List of plasmids used in this study

Name	Plasmids	Description	Sources
Vector	pRS416	Yeast shuttle vector	ATCC
GFP-Snc1 WT	pRS146-GFP-Snc1	GFP-tagged Snc1	Lewis, et al.2000(Lewis et al., 2000)
DUB-GFP-Snc1	pRS146-DUB-GFP-Snc1	Deubiqutinase(UL36) catalytic domain tagged GFP-Snc1	This study
DUB*-GFP-Snc1	pRS146-DUB*-GFP-Snc1	Catalytic dead form of deubiqutinase tagged GFP-Snc1	This study
GFP-Snc1-PM	pRS416-GFP-Snc1-PM	GFP tagged Snc1 with mutations in the Snc1 endocytosis signal	This study
DUB-GFP-Snc1-PM	pRS416-DUB-GFP-Snc1-PM	Deubiqutinase tagged GFP-Snc1-PM	This study
mCherry-Tlg1	pRS315-mCherry-Tlg1	mCherry tagged Tlg1	Xu, et al 2013(Xu et al., 2013)
3xHA-Snc1 WT	pRS416-3xHA-Snc1	3xHA tagged Snc1	This study
3xHA-Snc1 8KR	pRS416-3xHA-Snc1 8KR	3xHA tagged lysine-less Snc1	This study
3xFLAG-Ub	pRS315-3xFLAG-Ub	3xFLAG tagged Ub gene	This study
Myc-Emp47	pRS416-Myc-EMP47	N-terminal Myc tagged EMP47	This study
β'-COP WT	pRS315-SEC27	*SEC27* (β' COP) whole coding cassette including its promoter and terminator	This study
β'-COP RKR	pRS315-sec27 RKR	*SEC27* dilysine binding site mutant	This study
β'-COP Δ2-304	pRS315-sec27Δ2-304	*SEC27* with deletion the N-terminal β-propeller	This study
β'-COP human beta-Propeller	pRS315-hCOPB2(1-303)-sec(305-899)	*SEC27* first β-propeller replaced with human β'-COP propeller	This study
β'-COP UBD_{Doa1}	pRS315-Doa1(1-450)-Sec27(305-889)	*SEC27* first β-propeller replaced with DOA1(1-450)	This study
β'-COP NZF_{Tab2}	pRS315-NZF-Sec27(305-899)	*SEC27* first β-propeller replaced with NZF (TAB2 aa 665-693)	This study
α-COP WT	pRS313-COP1	COP1 whole coding cassette including its promoter and terminator	This study
α-COP Δ2-324	pRS313-cop1(325-1201)	COP1 deleting the first β-propeller	This study
human beta-Propeller-GST	pCOPB2(1-303)-GST	human β'-COP N-terminal propeller tagged with GST	This study
GFP-Rer1	pRS416-GFP-Rer1	GFP-tagged Rer1	(Sato et al., 1995)
Pib1-DUB	pRS416-CUP1-Pib1-DUB	DUB tagged Pib1	(MacDonald et al., 2017)

Tul1-DUB	pRS416-CUP1-Tul1-DUB	DUB tagged Tul1	(MacDonald et al., 2017)
Vps11-DUB	pRS416-CUP1-Vps11-DUB	DUB tagged Vps11	(MacDonald et al., 2017)
Rcy1-DUB	pRS416-CUP1-Rcy1-DUB	DUB tagged Rcy1	(MacDonald et al., 2017)
Rsp5-DUB	pRS416-CUP1-Rsp5-DUB	DUB tagged Rsp5	(MacDonald et al., 2017)
Pib1-DUB	pRS416-CUP1-Pib1-DUB*	DUB dead mutant tagged Pib1	(MacDonald et al., 2017)
Tul1-DUB	pRS416-CUP1-Tul1-DUB*	DUB dead mutant tagged Tul1	(MacDonald et al., 2017)
DUB-Rcy1	pRS313-DUB-Rcy1	DUB tagged Rcy1 in its N-terminus with Rcy1 promoter	This study
DUB*-Rcy1	pRS313-DUB*-Rcy1	DUB dead mutant tagged Rcy1 in its N-terminus with Rcy1 promoter	This study

Tables S2 List of strains used in this study

Name	**Genotype**	**Annotation**	**Sources**
BY4742	*MATα his3 leu2 ura3 lys2*	WT	Invitrogen
BY4742 YJL204C	*MATα his3 leu2 ura3 lys2 Rcy1::KanMX6*	RCY1 knockout	Invitrogen
ZHY615M2D	*MATα his3 leu2 ura3 lys2 drs2Δ::Kan*	DRS2 knockout	(Hua et al., 2002)
PXY46	*MATα his3 leu2 ura3 lys2 DRS2::UL36-3xHA::ClonNAT*	DRS2-DUB	This study
PXY47	*MATα his3 leu2 ura3 lys2 DRS2::UL36*-3xHA::ClonNAT*	DRS2-DUB C57S deadmutant	This study

KLY691	*Mata his3 leu2 ura3 gga1Δ::KanMX6 gga2Δ::KanMX6*	GGA pathway mutant	Invitrogen
BY4742 YPR029C	*MATα his3 leu2 ura3 lys2 apl4Δ::KanMX6*	AP1 pathway mutant	Invitrogen
BY4742 YPL195W	*MATα his3 leu2 ura3 lys2 apl5Δ::KanMX6*	AP3 pathway mutant	Invitrogen
BY4742 YJR058C	*MATα his3 leu2 ura3 lys2 aps2Δ::KanMX7*	AP2 pathway mutant	Invitrogen
EGY101-16d	*MATa ret1-1 leu2-3,112 ura3-52 his3-Δ200 trp1-Δ901 suc2-Δ9*	COP1 temperature sensitive mutant	(Gaynor and Emr, 1997)
PXY2174A	*MATα his3 leu2 ura3 lys2 sec27Δ::Hygro p315-SEC27*	SEC27 whole coding cassette	This study
PXY2175A	*MATα his3 leu2 ura3 lys2 sec27Δ::Hygro p315-sec27Δ2-304*	SEC27 deleting the first beta-Propeller	This study
PXY2186A	*MATα his3 leu2 ura3 lys2 sec27Δ::Hygro p315-sec27 RKR*	SEC27 dilysine binding site mutant	This study
PXY2193A	*MATα his3 leu2 ura3 lys2 sec27Δ::Hygro p315-hCOPB2(1-303)-sec(305-899)*	SEC27 first propeller replaced with human beta'-COP propeller	This study
PXY2184A	*MATα his3 leu2 ura3 lys2 sec27Δ::Hygro p315-Doa1(1-450)-Sec27(305-889)*	SEC27 the first beta-propeller replaced with DOA1(1-450)	This study
PXY2192A	*MATα his3 leu2 ura3 lys2 sec27Δ::Hygro p315-NZF-Sec27(305-899)*	SEC27 the first beta-Propeller replaced with NZF (TAB2 aa 665-693)	This study
PXY2198A	*MATα his3 leu2 ura3 lys2 cop1Δ::Hygro p313-COP1*	COP1 whole coding cassette	This study
PXY2199A	*MATα his3 leu2 ura3 lys2 cop1Δ::Hygro p313-cop1(325-1201)*	COP1 deleting the first beta-propeller	This study
PXY2100A	*BY4742 Cop1::mKate p313-GFP-Rer1*		This study
PXY2101A	*BY4742 Cop1::mKate p315-GFP-Tlg1*		This study
PXY2101C	*BY4742 Cop1::mKate p315-GFP-Tlg1*		This study
PXY2102A	*BY4742 Cop1::GFP::HIS3 Sec7::mKate::URA*		This study
PXY2103A	*BY4742 p416-GFP-Rer1 p313-mCherry-Tlg1*		This study
PLY5293	*BY4742 pib1Δ::KanMX6*	PIB1 knockout	Invitrogen
PLY5294	*BY4742 tul1Δ::KanMX6*	TUL1 knockout	Invitrogen

PXY64	*BY4742 pib1Δ::KanMX6 tul1Δ::mtx*	PIB1TUL1 double knockout	This study

References

Bolte, S., and F.P. Cordelieres. 2006. A guided tour into subcellular colocalization analysis in light microscopy. *J Microsc*. 224:213-232.

Chen, C.Y., M.F. Ingram, P.H. Rosal, and T.R. Graham. 1999. Role for Drs2p, a P-type ATPase and potential aminophospholipid translocase, in yeast late Golgi function. *The Journal of cell biology*. 147:1223-1236.

Gaynor, E.C., and S.D. Emr. 1997. COPI-independent anterograde transport: cargo-selective ER to Golgi protein transport in yeast COPI mutants. *The Journal of cell biology*. 136:789-802.

Hankins, H.M., Y.Y. Sere, N.S. Diab, A.K. Menon, and T.R. Graham. 2015. Phosphatidylserine translocation at the yeast trans-Golgi network regulates protein sorting into exocytic vesicles. *Mol Biol Cell*. 26:4674-4685.

Hua, Z., P. Fatheddin, and T.R. Graham. 2002. An essential subfamily of Drs2p-related P-type ATPases is required for protein trafficking between Golgi complex and endosomal/vacuolar system. *Mol Biol Cell*. 13:3162-3177.

Jackson, L.P., M. Lewis, H.M. Kent, M.A. Edeling, P.R. Evans, R. Duden, and D.J. Owen. 2012. Molecular basis for recognition of dilysine trafficking motifs by COPI. *Dev Cell*. 23:1255-1262.

Janke, C., M.M. Magiera, N. Rathfelder, C. Taxis, S. Reber, H. Maekawa, A. Moreno-Borchart, G. Doenges, E. Schwob, E. Schiebel, and M. Knop. 2004. A versatile toolbox for PCR-based tagging of yeast genes: new fluorescent proteins, more markers and promoter substitution cassettes. *Yeast*. 21:947-962.

Lewis, M.J., B.J. Nichols, C. Prescianotto-Baschong, H. Riezman, and H.R. Pelham. 2000. Specific retrieval of the exocytic SNARE Snc1p from early yeast endosomes. *Mol Biol Cell*. 11:23-38.

MacDonald, C., S. Winistorfer, R.M. Pope, M.E. Wright, and R.C. Piper. 2017. Enzyme reversal to explore the function of yeast E3 ubiquitin-ligases. *Traffic*.

Sato, K., S. Nishikawa, and A. Nakano. 1995. Membrane protein retrieval from the Golgi apparatus to the endoplasmic reticulum (ER): characterization of the RER1 gene product as a component involved in ER localization of Sec12p. *Molecular biology of the cell*. 6:1459-1477.

Silva, G.M., D. Finley, and C. Vogel. 2015. K63 polyubiquitination is a new modulator of the oxidative stress response. *Nat Struct Mol Biol*. 22:116-123.

Sobhian, B., G. Shao, D.R. Lilli, A.C. Culhane, L.A. Moreau, B. Xia, D.M. Livingston, and R.A. Greenberg. 2007. RAP80 targets BRCA1 to specific ubiquitin structures at DNA damage sites. *Science*. 316:1198-1202.

Stringer, D.K., and R.C. Piper. 2011. A single ubiquitin is sufficient for cargo protein entry into MVBs in the absence of ESCRT ubiquitination. *J Cell Biol*. 192:229-242.

Vida, T.A., and S.D. Emr. 1995. A new vital stain for visualizing vacuolar membrane dynamics and endocytosis in yeast. *J Cell Biol*. 128:779-792.

Xu, P., R.D. Baldridge, R.J. Chi, C.G. Burd, and T.R. Graham. 2013. Phosphatidylserine flipping enhances membrane curvature and negative charge required for vesicular transport. *J Cell Biol*. 202:875-886.

934 Yip, C.K., and T. Walz. 2011. Molecular structure and flexibility of the yeast coatomer as
935 revealed by electron microscopy. *J Mol Biol*. 408:825-831.
936